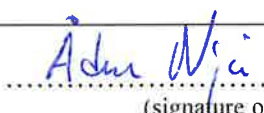# U S

Universitetet i Stavanger

FACULTY OF SCIENCE AND TECHNOLOGY

MASTER'S THESIS

Study programme/specialisation: Master of Science on Mathematics and Physics	Spring semester, 2019 Open
Author: Ådne Njå	*Ådne Njå* .... (signature of author)

Programme coordinator:

Supervisor(s):   Professor Jan Terje Kvaløy and Professor Per Amund Amundsen

Title of master's thesis:

Modelling fire occurrences in heavy goods vehicles in Norwegian road tunnels

Credits: 60

Keywords: Poisson regression models Tunnel fire incidents Tunnel slope Subsea tunnel Tunnel length AADT HGV	Number of pages: 90 + supplemental material/other: .... Stavanger,15.06.2019 date/year

Modelling fire occurrences in heavy goods vehicles in Norwegian road tunnels

Ådne Njå

June 15, 2019

Abstract

This master thesis project has been organized to scrutinize current incident data on near fires and fully developed fires in Norwegian road tunnels longer than 500 meter. This length is chosen because it is assumed that this length could threaten humans in case of fires. There has been a huge effort in collecting data and transfer them into formats that has enabled mathematical modelling. The major issue of this thesis have been to resolve; What are the major contributing tunnel infrastructure factors leading to heavy goods vehicles fires in Norwegian tunnels? By using Poisson regression modelling several models are developed showing good fit with the observations. All models revealed that slope, length, annual average daily traffic of heavy goods vehicles, and whether a tunnel is subsea, are the significant factors. The most important factor is the subsea factor. This interacts with certain other factors revealing that subsea tunnels with excessive attributes are really exposed to HGV fires. The thesis discusses weaknesses in the data material, as well as there are a number of other interesting factors, for example related to the state of HGVs and driver behavior that are currently missing. The research potential is huge in order to improve the models and the understanding of HGV fires in tunnels.

Preface

When the idea of modelling the development of HGV fires in tunnels first became an issue, my approach was to understand the physics and thermodynamics from the HGVs entered the tunnels until the fire occurred. I soon realized that current data and possibilities to reveal necessary data was impossible. However, the best data available was handed over by all parties approached. I will take this opportunity to thank Tor-Olav Nævestad, TØI for his good service and providing all his data, and the NPRA, Arild Engebretsen, for the roadmap. I have also followed up every tunnel that had lacking data with several people, not being named – thanks for the contribution.

I needed to understand the challenges the truck drivers experience when driving in tunnels. I therefore approached Reidar Mikkelsen, who included me in one of his YSK-courses. Reidar also provided information from his lectures of fresh truck drivers. Thank you Reidar!

We also visited SR Transport in Rogaland in order to visually inspect trucks and the potential hot surfaces of a truck. Our guide was Øystein Lundmo. Thank you Øystein for your very informative and thoughtful introduction.

At the University of Stavanger I have been so lucky to become supervised by Professor Per Amundsen and Professor Jan Terje Kvaløy. Your contribution to my project is deeply acknowledged and valued. The systematic and thorough meetings with you have learnt me a lot during the process.

Abbreviation	Meaning
NPRA	Norwegian Public Road Authorities
DSB	Directorate of Civil Protection
TØI	Institute of Transport economics (Trasportøkonomisk institutt)
AIBN	The Accident Investigation Board Norway
HGV	Heavy goods vehicle
AADT	Annual average daily traffic
AIC	Akaike information criterion

Table 1: List of Abbreviations

Contents

1   Introduction

Studying real world phenomena related to complex systems using mathematics is challenging. This thesis assesses fire risks in Norwegian road tunnels focusing on fire occurrences.

1.1   Framing the issue

Norway has more than 1200 road tunnels, which have been erected and put in operation from the year 1891 (Eidfjord tunnel), and there are still many tunnels under construction. Their designs vary from single tube "black holes" to dual tube fully equipped tunnels addressing high quality safety considerations. Tunnels are elements of the road transport infrastructure in Norway, which is also of a varied quality.

However, Norway is amongst the safest countries in the world when we regard risk of traffic accidents termed Zero Vision accidents (Langeland, 2009). These accidents are characterized by fatalities or seriously injured victims. The consequence categories are internationally agreed upon, but Elvik and Mysen (1999) have documented weaknesses in the reporting systems. Weaknesses are also confirmed by Njå, Jakobsen and Nesvåg (2008). Even though there might be differences in the traffic accident statistics between countries, the statistics of the Zero Vision accidents are more reliable than less serious accidents.

Statistics of incidents in tunnels encompassing near fires and fires in heavy goods vehicles (HGVs) should also be carefully considered. We will discuss more thoroughly the current statistics in the thesis (Section 8). Regarding major fire events, for example seen in Europe approximately twenty years ago (Mont Blanc, Tauern and St. Gotthard tunnels), Norway has not seen such events. The fire accidents in Norway have not included fatalities from smoke intoxication. Since 2011 Norway has experienced a number of HGV fires, which under different circumstances very easily could have developed into cascades as seen in Europe.

The Norwegian Public Administration (NPRA) has been the owner and regulator of the tunnels in Norway. This is about to change, in which the county governments are now owners of a major population of the road infrastructure.

The designs of tunnels must be seen as part of the road sections, to which they belong. The historical development of technologies, traffic safety criteria and international regulation are also important. Many of the older Norwegian single tube tunnels are part of an EU induced upgrading programme, which will be finalized in few years (the original plan was 2019). Still, this programme will neither not provide standardized solutions, thus it must be expected that the variety of the tunnel designs also influence risk of accidents.

Njå and Kuran studied the fire in the Oslofjord tunnel in 2011 (Njå and Kuran, 2015). They recommend that tunnel fire safety should be improved in Norway, based on various characteristics with the tunnel design that emerged in the study:

- It takes too long time before road-users realize dangerous situations in tunnels and prepare for self evacuation.

- The organizing of self-evacuation is arbitrary and to a very little extent adapted for the road-users needs.

- The road-users do not possess knowledge of tunnel fires.

- The buyer of transport services, transport salesmen, forwarding agents, transport companies and drivers of HGVs containing large amount of energy has been very little considered and scrutinized with respect to their roles and responsibilities regarding major fires in tunnels.

- Knowledge of fire dynamics, heat development and smoke dispersion in tunnels is weak.

- Easy accessed information about Norwegian road tunnels and fire protection strategies is lacking.

- The individual victims' post traumas and stresses is underrated.

1.2 The need for modelling tunnel characteristics leading to HGV fires

The potential for severe accidents (> 5 fatalities) stems from HGV fires not being controlled and/or containing toxic substances either as dangerous goods or from fire effluents. The fire ventilation strategy for Norwegian tunnels is longitudinal with high velocities transporting the smoke that includes toxic fire effluents with velocities of 3 m/s and higher. The air flow

is from the tunnel entrance with the prominent fire department towards the other side regardless of where in the tunnel the fire occurred. The two fires in the Gudvanga tunnel (2013 and 2015) both included transport of smoke over large sections, more than 8 kilometers. Some victims were engulfed in smoke for approximately 90 minutes before reaching the entrance or being rescued by first responders.

Exposure to toxic fire smoke and gases (Stec and Hull, 2010) cause injuries and deaths in fires. The traditional terms of assessing fire safety of humans are connected with the outcome of two parallel timelines. These are the time from ignition of the fire to the development of incapacitating conditions (ASET) and the time required for tunnel users to reach a place of safety (RSET) (Bjelland and Njå, 2012; Hurley, 2016). When occupants become immersed in smoke, behavioural, sensory and physiological effects occur. Toxic fires effluents are responsible for the majority of fire deaths and an increasingly large majority of fire injuries (Stec and Hull, 2010). According to Lönnermark's opinion (Lönnermark, 2007), there must be cascading accident if HGV fires in tunnels shall be fatal.

Current research and state of the art regarding tunnel fire safety are mostly concerned with conditions after ignition and how the fire dynamics affect structures, equipment, and rescue and evacuation conditions (Carvel and Beard, 2005; Ingason, Li and Lönnemark, 2014). This research yields fire dynamics, fire ventilation, evacuation systems and behavior and fire extinguishing technologies that have been explored using various perspectives and research designs. Tunnel fire risk assessments encompass estimated fire frequencies, but these frequencies are rough estimates mostly based on "engineering judgements", thus no in depth evidence on why and how fires occur are normally included in such analyses.

Accident investigations are also very scarce on showing solid evidences of why and how fires occur, and which factors that contribute to the ignition and sustained fires in HGVs. This is quite odd when we consider the vast experiences with Norwegian risk management practices that emphasize knowledge based assessments and risk reducing measures prioritizing fire prevention. In Switzerland, at the entrances of the St. Gotthard tunnel, the tunnel owner has installed assemblies of temperature sensors monitoring hazardous conditions in HGVs before entering the tunnel. However, the knowledge is lacking. In this master thesis work we had a prior ambition to model physics and thermodynamics in HGVs from entering the tunnel to

ignition occur. We soon realised during information gathering that this task would not be possible during a master thesis, so we then wanted to explore all Norwegian tunnel fire data in order to establish a model of the tunnel characteristics contributing to the risk of HGV fires. The major issue then became;

What are the major contributing tunnel infrastructure factors leading to HGV fires in Norwegian tunnels?

The Norwegian regulations on tunnel safety have been developed from the 1980-ies, when the first challenging subsea tunnels was planned and constructed. A specific handbook (SVV, 2006) became the governing tool for planners involved in tunnel projects. The regulation was prescriptive with detailed requirements to geometry, materials and safety equipment. In the 1990-ies there were critical voices addressing toxic insulation materials and less effective concrete linings (Dahle, 2005). Towards the millennium, the catastrophic tunnel fires in Europe triggered regulatory game changes, which were implemented through the Directive 2004/54/EC (2004) on minimum safety requirements for tunnels in the Trans-European Road Network. The period included much research work and tunnel safety was strengthened in regulations. Now the safety considerations should be systematically approached from risk assessments, the tunnel owner appointing safety officers, establishing administrative authorities, safety documentation etc.

The Norwegian tunnels in operation did not comply with the requirements and neither did the regulations. Handbook 021 (SVV, 2006) was updated several times, the last time in 2016. The current format has status as a regulation (SVV, 2016), being a legal document. The current Norwegian regulations are adapted to the European directives and the NPRA claims that they have enhanced safety precautions, through risk informed designs. Important constraints are tunnel slope $< 5\%$, emergency walkways, drainage for flammable fluids, lighting, ventilation, monitoring systems, communication systems, emergency power supply and fire resistance of equipment. However, current knowledge about the conditions of HGVs using Norwegian tunnels, and how and why fires occur are scarce. This thesis must be seen as commencing the work to understand fire occurrences in tunnels.

1.3 Structure of thesis

In section 2 we discuss briefly how and where the data material was collected. In section 3 we explore AIBNs investigations of fire in HGVs in tunnels. In section 4 we discuss the information received from an experienced truck driver. We use this information to define hot surfaces within the truck and the source of ignition. In section 5 we model the mechanical components of a heavy goods vehicle in motion on an inclined plane. In section 6 we introduce heat transfer from thermodynamics, and discuss the validity of experimental measurements of heat transfer in diesel engines. In section 7 we introduce the theory of regression model and all its aspects which are later used in section 8 where we model fire in HGVs in road tunnels. In section 9 we examine certain subgroups of the whole data material to see if the circumstances are the same in interesting subgroups compared to the entire dataset. In section 10 we compare certain models to find the best model which is presented in section 11.

2   Incident data employed in study

We accessed all data material available from the Norwegian Public Roads Administration (NPRA), the Institute of Transport Economics (TØI), the Directorate for Civil Protection (DSB) and the Accident Investigation Board Norway (AIBN). This material does not contain records on driver behaviour or technical conditions of the vehicles involved. Hence, the work consisted of developing models from tunnel characteristics and traffic flow.

The data has been accumulated such that almost every road tunnel in Norway longer than 500m is included. For each tunnel, we have gathered data on 11 different variables. These are variables that we expect will influence fire accidents in road tunnels. TØIs data on accidents has been used to count fire and near fire incidents in HGVs in road tunnels. Other variables such as slope, length and annual average daily traffic (AADT) has been obtained in NPRAs data material. For a more explicit summary of the data collection, see section 8.1.

TØI has conducted a mapping of all fire accidents in Norwegian road tunnels from 2001-2015 (Nævestad, 2016). Nævestads data shows that it occurs on average 4.8 fires in HGVs each year in Norwegian road tunnels. Table 2 shows the number of fully developed HGV fires that occurred each year due to technical failure.

Year	Fire in HGVs	Year	Fire in HGVs
2001	1	2009	3
2002	0	2010	9
2003	4	2011	6
2004	4	2012	6
2005	3	2013	7
2006	7	2014	11
2007	1	2015	6
2008	4	Total	72

Table 2: Fully developed fires in HGV in tunnels from 2001 to 2015

They are distributed like this (Njå, 2017):

- Region east - 19 fires in HGVs in 15 years, of which 7 in the Oslofjord tunnel and 5 in the Opera tunnel, while the last 7 were in different tunnels.

- Region south - 8 fires in HGVs in 15 year divided into different tunnels.

- Region west - 30 fires in HGVs in 15 year, of which 5 in the Mastrafjord tunnel and 3 in Gudvanga tunnel, while the last 22 were in different tunnels.

- Region middle - 8 fires in HGVs in 15 years, of which 4 in the Hitra tunnel and 2 in the Eiksund tunnel, while the last 2 were in different tunnels.

- Region north - 7 fires in HGVs in 15 years divided into different tunnels.

It may be important to analyse cases where fire has not yet been fully developed. If we include these cases, the data from Nævestad shows that it occurs on average 9.4 fires in HGV each year in Norwegian road tunnels. Table 3 shows the number of HGV fires and near fires that occurred each year due to technical failure.

Year	Fire/near fire in HGVs	Year	Fire/near fire in HGVs
2001	1	2009	7
2002	0	2010	13
2003	7	2011	18
2004	7	2012	11
2005	6	2013	16
2006	9	2014	19
2007	3	2015	13
2008	11	Total	141

Table 3: Both fire development and fully developed fires in HGVs in tunnels from 2001 to 2015

They are distributed like this (Njå, 2017):

- Region east - 36 fire in HGVs in 15 years, of which 12 in the Oslofjord tunnel, 6 in the Opera tunnel and 4 in the Ekeberg tunnel, while the last 14 were in different tunnels.

- Region south - 12 fire in HGVs in 15 year divided into different tunnels.

- Region west - 65 fire in HGVs in 15 year, of which 11 in the Byfjord tunnel, 6 in the Bømlafjord tunnel, 7 in the Mastrafjord tunnel and 5 in the Gudvanga tunnel, while the last 36 were in different tunnels.

- Region middle - 21 fire in HGVs in 15 years, of which 5 in the Hitra tunnel and 4 in the Eiksund tunnel, while the last 12 were in different tunnels.

- Region north - 7 fire in HGVs in 15 years divided into different tunnels.

We can see from the tables in both cases that there is a large variance in data. There were a lot less accidents in the years 2001-2007 compared to 2008-2015. We can ask the question; why? Is it because drivers were better before? Has the quality of the newer trucks worsen? Were there better regulations of maintenance? Can the reason be that there were more vehicles on the road in 2008-2015 compared to 2001-2007? Or is it because we have become better at reporting accidents? These are some possible explanations for the increased accident rates.

It has not been any attempt to analyse connections between near fires and fully developed fires. Whether the near fires is a good indicator for evaluating the probability of fire in heavy goods vehicles (Njå, 2017), needs further studies.

3 AIBNs investigations of HGV fires in tunnels

The Accident Investigation Board Norway (AIBN) has investigated six different fires in HGVs in tunnels. As only a handful of incidents have been properly investigated, it is important that we explore the rich data material from AIBNs investigation and discuss their results.

3.1 Oslofjord tunnel 5. May 2017

On 5 May 2017, a fire broke out in a Latvian registered heavy goods vehicle on the way up the 7% incline towards Drøbak in Oslofjord tunnel. There were in total 127 vehicles inside the 7.3km long Oslofjord tunnel when the accident occurred. The fire occurred as a result of an engine breakdown, approximately 5 km in to the tunnel from the entrance. AIBN (2018) has investigated the accident and found that the engine broke down as a result of one of the connecting rods penetrated the engine room. A monitoring camera in the Oslofjord tunnel revealed the red hot rod in the lane just as the incident occurred. AIBN concluded that one of the oil supply cylinders to the connecting rods broke out of position. This partly reduced the oil flow to the connecting rods. Once the vehicle got to the bottom of the Oslofjord tunnel and started climbing the tunnel again, more load were required on the rods, the rpm increased, and without oil supply, the rods were not lubricated. Consequently, the connecting rod got extremely hot due to friction between metals, and the rods bearing evidently shattered. The rod were shot through the engine room, and caused a big hole of 14 cm in diameter. This further caused damage to the vehicles fuel system, and the leaking fuel ignited inside the broken engine.

3.2 Oslofjord tunnel 23 June 2011

On 23 June 2011 a Polish registered lorry truck caught fire on the way up the 7% incline towards Drøbak in Oslofjord tunnel. According to AIBN (2013), the fire occurred as a result of an engine breakdown, almost identically to the accident in 2017. The accidents occurred at almost the same location, just 500m apart. In both cases, the bearing of the rod shattered and penetrated the engine room as a result of limited oil supply and increased friction between metals.

3.3 Gudvanga tunnel 5 August 2013

On 5 August 2013, a Polish registered heavy goods vehicle caught fire inside the 11.4km Gudvanga tunnel. There were in total 58 vehicles inside the Gudvanga tunnel when the accident occurred. AIBN has not been able to establish exactly why the vehicle caught fire. However, AIBN found several factors that may have contributed to fire ignition. According to their report (AIBN, 2015), these factors are;

- Wear damage on protective braiding around the oil line between the oil cooler and turbo.

- Traces of short-circuiting in several of the vehicle's electrical wires.

- A hole in the throttle housing for the engine break (on the turbine side of the turbo). The hole was on the side that faced the engine.

- Melting damage to the rear part of the dynamo with diode bridge and connections.

Exactly which factor sparked the ignition has been impossible to establish, based on the technical examination. 67 people were trapped inside the tunnel, 23 were seriously injured and 5 were very seriously injured, though there was no fatalities.

3.4 Gudvanga tunnel 11 August 2015

On 11 August 2015, a tourist coach caught fire inside the 11.4km Gudvanga tunnel. According to the AIBN (2016a) investigation, they were not able to determine what exactly caused the fire ignition. However, the technical examination revealed a leakage in the cooling system, clogged cooling fins in the radiator, and worn splines in the hydraulic pump. These factors may have caused a temperature increase in the engine compartment, and AIBN believes this further caused the fire ignition. Furthermore, AIBN believes the failure in the engine compartment occurred before the vehicle entered the Gudvanga tunnel, and the incident could have been prevented had the bus driver detected the fire before the bus entered the tunnel. 5 people were trapped in the tunnel filled with smoke. They were all evacuated and taken to the hospital.

3.5 Skatestraum tunnel 15 July 2015

On 15 July 2015, a tank trailer containing petrol hit the tunnel wall in the Skatestraum tunnel. There were in total 5 vehicles inside the 1.9km

long Skatestraum tunnel when the accident occurred. The material that connected the trailer and the tank were severely reduced due to an advanced state of internal corrosion (AIBN, 2016b). This further caused the front of the tank to hit the wall and large volumes of petrol began to leak out of the tank. Because of the steep gradient of the tunnel, the patrol quickly ran down to the bottom of the tunnel. The SP Technical Research Institute of Sweden has studied possible sources of ignition. They believe the petrol vapour was ignited by hot surfaces or sparks from the electrical system within one of the vehicles that were inside the tunnel at the time, most probably a camper van. According to SPs calculation, the maximum heat release rate within the tunnel exceeded 400MW, and the temperature above the burning trailer was approximately $1350°C$ (AIBN, 2016b).

The investigation revealed a leakage in one of the tunnels water pipes that caused petrol to run in to the water system. This meant that both the petrol on the tunnel surface and in the water system was on fire.

Because of the vast heat and smoke within the tunnel, the accident inspectors were not able to enter the tunnel before 6 days after the accident.

17 people distributed in 5 vehicles were inside the tunnel when the accident occurred. Everyone managed to evacuate the tunnel.

3.6 Måbø tunnel 19 May 2016

On 19 May 2016, a heavy goods vehicle carrying an excavator caught fire on the way up the 9.9% incline towards Gol inside the Måbø tunnel. The total weight of the vehicle were 71 tons. Just a few hundred meters inside the Måbø tunnel, the driver noticed smoke exhaust coming from the vehicle.

AIBN (2017) technical investigation revealed a hole in one of the damaged hoses connected to the vehicle's hydraulic system. The vehicles weight condition and stress is believed to have caused the hoses to rub against each other and eventually rip a role in one of them. This further caused hydraulic oil to leak. The leakage caused hydrolic oil to come in contact with hot surfaces within the vehicle, and AIBN believes this is the reason that caused fire ignition.

3.7 Discussion

The statistical modelling in Section 7-11 reveal 4 significant variables influencing the rate of fire accidents in road tunnels. A common aspect of all tunnels investigated by AIBN is that all of them have atleast one distinct tunnel characteristic significant for fire in HGVs.

For a more detailed overview of significant variables, and why these tunnels seems to be more exposed to HGV fires, see section 12.

Moreover, remarkably many fire accidents investigated by AIBN has included a foreign vehicle. An informant of a transport company claimed that many of the foreign HGVs coming to Norway were not fit for Norwegian terrain. In particular, they often lack design and maintenance.

4 Introduction to heavy goods vehicles seen from a fire occurrence perspective

This chapter is based on the author attending a mandatory refreshment course for professional truck drivers (YSK – yrkessjåførkurset), provision of curricula and presentation from modules of other basic courses for professional truck drivers. We have visited a local experienced transport company that have been involved in transport services for the oil & gas industry for many decades. Our aim was to visually inspect the systems of the truck, together with an experienced employee also being a lecturer for professional truck drivers.

The literature review revealed that phenomena related to fires in HGVs in tunnels are superficially recorded and treated, even in the AIBN investigations. Thus, we found that an in-depth discussion of the critical systems in the heavy goods vehicles are of less importance since it will not be used in the research work. But, most fires occur due to malfunctions in the critical systems, but without any knowledge of the prior conditions in the vehicles. The fire quadrangle serves as a starting point for this introduction to components and systems in heavy goods vehicles, placing weight onto the fuel and temperature parameters under conditions that oxygen is present. The catalyst premise (chain reaction) is less considered in this presentation. Fires due to collisions are a special case, which is not pursued in the thesis.

The research institute RISE gives bi-annually conferences on fires in vehicles (FIVE), which could have served as a background, cf. *FIVE* (2019). A review of the papers that have been presented does not provide scientific results on either the condition of the HGV population entering tunnels nor causes and models for fire occurrences; we also refer to the previous chapters.

The presentation is system wise, discussing the engine, fuel, exhaust and cooling systems, the brake systems, and miscellaneous that might contribute to fire occurrence.

4.1 Engine, fuel, exhaust and cooling systems

Most trucks use diesel engines due to its superior power efficiency. The diesel engine, of which principles is depicted in figure 1 is a self-ignition engine. Air is compressed, pressure and temperature increases, diesel oil is sprayed in and ignites to produce the work-tact. The ignition temperature of diesel

is approximately $200°C$. Trucks with relevant total weight of more than 40 tons needs to be equipped with a 280 hp (206 kW) engine.
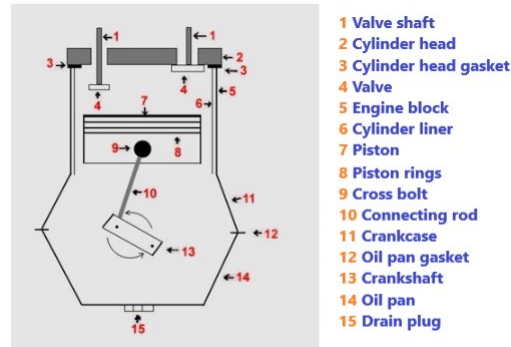

Figure 1: Engine, Mikkelsen (2018)

The introduction of eco-diesel has lowered the ignition temperature, which represents an increased fire hazard from leakages. Electronic fuel injection increases accuracy and optimize the working loads of the engines. Lube oil and cooling systems both ensures that the engine operates within tolerable limits and avoids high temperatures. Malfunctions, wearing and failures in these systems have provided fire occurrences, either as hot surfaces igniting fuel material in its surroundings, or sudden damages leading to breakages of pipes and hoses containing substances that ignites at lower temperatures. The exhaust systems contains gas in elevated temperatures that is also a hazard if there is malfunctions in the insulation design. In addition to traditional petrol based engines, now new fuel systems, such as electric motors and hydrogen-based motors will change current challenges seen from the HGV fires.

Figure 2: In front and behind the vehicle examined

4.2 The brake system

The operating brake system has a transmission device that can be mechanical, hydraulic, pneumatic or electric. There are three arrangement of brakes;

- Friction type: Drum brake and disc brake

- Electric type: Eddy current brake, also known as electric retarder. Unlike friction type brakes, eddy current brake uses electromagnetic force between a magnet and a conductor in a relative motion to decelerate the vehicle

- Fluid type

Figure 3: Wheel bearings and retarder

Defect brakes on some shafts/wheels introduce instabilities, which are a fire hazard. The informant (experienced performer) from the transport company claimed that many of the foreign HGVs coming to Norway were not fit for purpose, both the designs (e.g. two-axl, tires) and the maintenance level. However, he said that the situation seemed now to be improved amongst the foreign HGVs.

4.3   Miscellaneous

So far we have introduced major systems that are obvious candidates for fire occurrences. Nevertheless, fires are always a compound of several factors that includes how the systems are operated, maintained and constructed. Design weaknesses are also part of this. For example, there might be spaces between the carrier and the engine room that enables substances easily ignited to enter the engine room. The experienced performer referred to an event related to transporting wood chips, in which the chips in the engine room caught fire. He was pointing to the truck driver's role in the driving conduct as a major contributor to fire occurrences, but he maintained that the management systems involved and the frameworks for carrying out the transport should ensure optimal conditions for the drivers. In general, the experienced performer claimed that dirt in the engine room is a major contributor to fires, both as a contaminator prohibiting cooling as well as it containing oil and other substances that constitute fire hazards.

Figure 4: Motor and exhaust pipe

The electrical systems are a fire hazard, either from erroneous use, from damaged insulation or junctions, or components such as the dynamo. The engine room is filled with polymer-based products and rubber hoses that will sustain fires once occurred.

Leakages of hydraulic fluids, lube oils, diesel oils are critical. Some of the fuel systems contain high pressures that could worsen the situation after ignition. Fires might develop very fast.
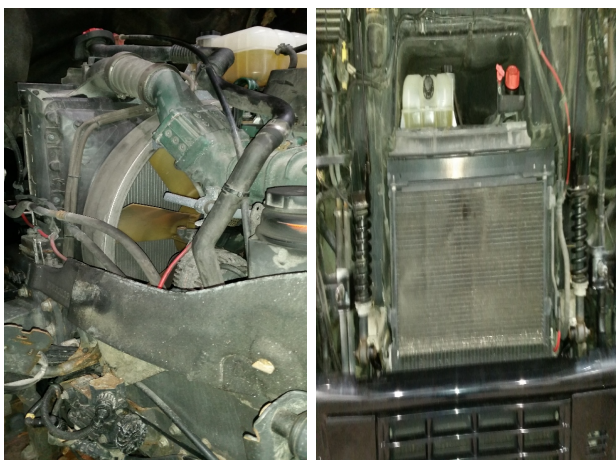
Figure 5: Air fan and radiator

Wheel bearings are another area that might provide heated zones and fire occurrences in tires and surrounding substances. Tires might also catch fires in certain conditions. The wheel areas containing shafts, half-shafts, sun wheel, brakes, bearings and tires are complex and need to be carefully considered as a fire hazard. A diesel storage tank of approx. 500 liters also contribute to the risk image of fire occurrences in HGVs.

5   Mechanical modelling

In this section, we will analyse the mechanical forces that are in place when a heavy is vehicle driving through an inclined tunnel. First and foremost, we need to know what forces acts on a vehicle driving downwards and upwards an inclined plane. There will be three forces acting on the vehicle both downwards and upwards:

- The force of gravity

- Drag force

- Rolling resistance

Gravitational force
From basic trigonometry we see that the gravitational force acting on the vehicle along the hypotenuse is

$$F_g = mg\sin(\theta)$$

where m is the mass of the vehicle, g is the gravitational constant (9.8m/s^2) and θ is the angle of the incline.
Drag force
Drag force is a resistive force due to an object moving through a fluid and is derived from Newton's drag equation.

$$F_d = \frac{1}{2}\rho v^2 C_d A$$

where

- ρ is the density of the fluid

- v is the velocity of the object relative to the fluid

- C_d is the drag coefficient

- A is the cross sectional area of the object

The drag coefficient is a dimensionless constant and depends, in general, on the Reynolds number Re. The Reynolds number is the ratio of inertial and viscous forces in the fluid.

Laminar flow, which is highly ordered fluid motion has a low Reynolds number. Turbulent flow, which is highly disordered fluid motion has a high

Reynolds number.

HGVs moves rather quickly, and the motion of HGVs moving through air is therefore considered turbulent. At higher Reynolds numbers, the drag coefficients for most geometries remain essentially constant (Cengel, Cimbala and Turner, 2012). Thus, we can use drag coefficient for HGVs found in tables.

The density of air, ρ, is not constant throughout the tunnel as it depends on temperature and pressure. But we assume this difference is practically negligible.

Rolling resistance
Rolling resistance is a force resisting the motion when a wheel is rolling on a surface.
$$F_r = C_{rr}N$$
where

- C_{rr} is the rolling resistance coefficient

- N is the normal force perpendicular to the surface

The normal force of an object on an inclined plane is $N = mgcos(\theta)$. This means that the rolling resistance of a vehicle moving on an inclined plane is

$$F_r = C_{rr}mg\cos(\theta)$$

Although each of these forces are equal in magnitude for both down and up the inclined plane (given the same conditions), they are not necessarily in the same direction. The force of gravity will always point towards the center of the earth, meaning it will accelerate the vehicle on the way down and decelerate the vehicle on the way up. Both drag force and rolling resistance will act in the opposite direction of motion, meaning it will decelerate the vehicle both on the way up and down, see figure 6.
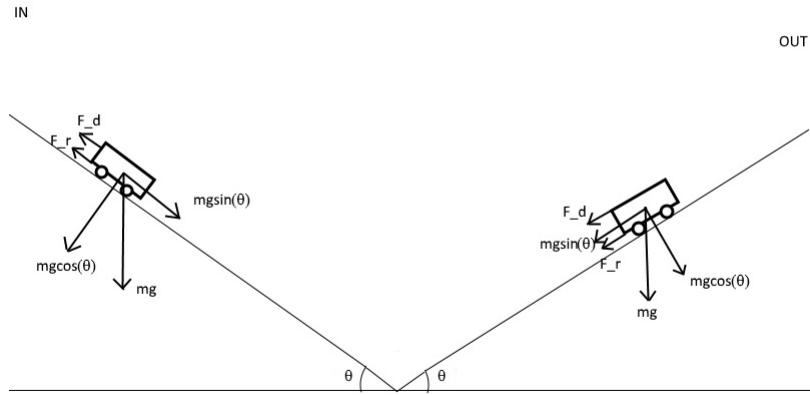
Figure 6: Different forces acting on a vehicle ascending and descending an inclined plane

Downward motion

In order for the vehicle to drive with constant velocity, the net force acting on the vehicle parallel to the road surface has to equal zero.

$$F_g - F_d - F_r - F_b = 0$$

where

- F_g is the force of gravity

- F_d is the drag force

- F_r is the rolling resistance

- F_b is the break force

Solve the equation for F_b

$$F_b = F_g - F_d - F_r$$

$$F_b = mg\sin(\theta) - \frac{1}{2}\rho v^2 C_d A - C_{rr} mg\cos(\theta)$$

$$= mg\big(\sin(\theta) - C_{rr}\cos(\theta)\big) - \frac{1}{2}\rho v^2 C_d A$$

The break power needed to keep a vehicle with constant velocity moving down an inclined plane is

$$P_b = F_b v = mgv\big(\sin(\theta) - C_{rr}\cos(\theta)\big) - \frac{1}{2}\rho v^3 C_d A$$

The energy, or work, required by the brakes is

$$W_b = \int_0^x F_b\, dx$$

x being the displacement along the hypotenuse and depends on the vertical and horizontal lengths, as well as the angle. Solve the integral to obtain a function for work;

$$W_b = \int_0^x \left(mg\big(\sin(\theta) - C_{rr}\cos(\theta)\big) - \frac{1}{2}\rho v^2 C_d A\right) dx$$

$$W_b = mgx\left(\sin(\theta) - C_{rr}\cos(\theta)\right) - \frac{1}{2}\rho v^2 C_d A x \qquad (5.1)$$

Upward motion

Newtons law of motion also applies for a vehicle driving up an inclined plane. Only this time, the resistive forces acts in the same direction as the force of gravity

$$F_g + F_d + F_r - F_e = 0$$

where F_e is the engine force. Solve for F_e

$$F_e = mg\big(\sin(\theta) + C_{rr}\cos(\theta)\big) + \frac{1}{2}\rho v^2 C_d A$$

The engine power needed to go up the inclined plane is

$$P_e = F_e v = mgv\big(\sin(\theta) + C_{rr}\cos(\theta)\big) + \frac{1}{2}\rho v^3 C_d A$$

And to do so, the engine requires an energy of

$$W_e = \int_0^x \left(mg\big(\sin(\theta) + C_{rr}\cos(\theta)\big) + \frac{1}{2}\rho v^2 C_d A\right) dx$$

$$W_e = mgx\Big(\sin(\theta) + C_{rr}\cos(\theta)\Big) + \frac{1}{2}\rho v^2 C_d Ax \qquad (5.2)$$

Now let us consider two examples. We will see how the total energy required by the engine and the brakes depend on the tunnel angle. We first fix its height and then its length, respectively.

Example 1 (fixed height)

Suppose a truck weighing 50 tons drives through an inclined tunnel with a velocity of 80 km/h. The resistive coefficients of a typical truck are $C_{rr} = 0.005$ and $C_d = 0.6$. Assume the cross sectional area of the truck is $A = 10m^2$ (2.5m wide and 4m height). The density of air depends both on pressure and temperature, but we will use the density of air at 1 atm and $20°C$, $\rho = 1.225$, for this purpose. We will also consider the the vertical length of the bottom of the tunnel compared to the entrance to be 200m. Given these conditions, we can evaluate both engine and brake work as a function of the angle.

By basic trigonometry, we can find the length of the hypotenuse, x, as a function of the angle.

$$\sin(\theta) = \frac{h}{x}$$

$$x = \frac{h}{\sin(\theta)} \qquad (5.3)$$

By substituting equation 5.3 into equations 5.1 and 5.2, we get the break and engine work as a function of θ.

Break work:

$$W_b(\theta) = mgh\Big(1 - \frac{C_{rr}}{\tan(\theta)}\Big) - \frac{\rho v^2 C_d Ah}{2\sin(\theta)}$$

$$W_b(\theta) = \Big[98\big(1 - 0.005\cot(\theta)\big) - 0.363\csc(\theta)\Big]\text{MJ} \qquad (5.4)$$

Engine work:

$$W_e(\theta) = mgh\Big(1 + \frac{C_{rr}}{\tan(\theta)}\Big) + \frac{\rho v^2 C_d Ah}{2\sin(\theta)}$$

$$W_e(\theta) = \Big[98\big(1 + 0.005\cot(\theta)\big) + 0.363\csc(\theta)\Big]\text{MJ} \qquad (5.5)$$
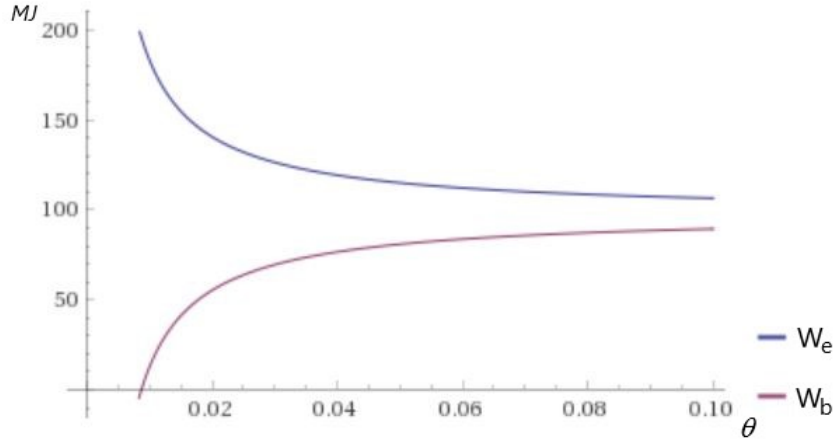
Figure 7: Engine work and brake work as a function of θ with fixed height.

Example 2 (fixed length)

Let us consider the same truck with the same conditions, only this time we fix the horizontal distance from the entrance to the exit of the tunnel to be $l = 6000m$. Then

$$x = \frac{l}{2\cos(\theta)} \qquad (5.6)$$

By substituting equation 5.6 into equations 5.1 and 5.2, we get the break and engine work as a function of θ

Break work:

$$W_b(\theta) = \frac{mgl}{2}(\tan(\theta) - C_{rr}) - \frac{\rho v^2 C_d A l}{4\cos(\theta)}$$

$$W_b(\theta) = \big[1470(\tan(\theta) - 0.005) - 5.44\sec(\theta)\big]\text{MJ} \qquad (5.7)$$

Engine work:

$$W_e(\theta) = \frac{mgl}{2}(\tan(\theta) + C_{rr}) + \frac{\rho v^2 C_d A l}{4\cos(\theta)}$$

$$W_e(\theta) = \big[1470(\tan(\theta) + 0.005) + 5.44\sec(\theta)\big]\text{MJ} \qquad (5.8)$$
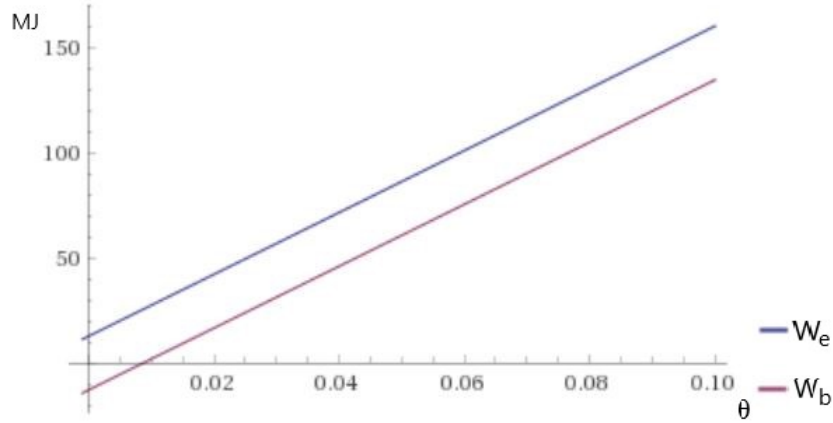
Figure 8: Engine work and brake work as a function of θ with fixed length.

As we can see from figure 8, both W_b and W_e are almost linear. This is because $\tan(\theta) \simeq \theta$ and $\cos(\theta) \simeq 1$ when $\theta << 1$.

Conclusion:
In example 1, the total energy required by the brakes and engine approaches $\pm\infty$ as $\theta \to 0$. This is because there will always be some energy lost due to resistive forces along the way and when the length of the hypotenuse approaches ∞ as $\theta \to 0$, the energy lost also approaches ∞. The same argument goes for example 2 as $\theta \to \frac{\pi}{2}$. Although, we are not interested in these limits as they are not practical. We are interested in $\theta \in [1, 10]\%$ inclination, and so we should exclude all other values of θ.

6   Heat Transfer

This section is based on Cengel et al. (2012) and Drysdale (1999)

As we have seen in Section 5, the magnitude of mechanical energy that is produced either in the brakes or the engine is huge. How is the energy transformed? Often when an accident occur, it is related to some surface inside the truck becoming extremely hot. If this hot surface comes in contact with a combustible material (e.g fuel or hydraulic fluid), it may spark a flame. How can we describe the heat of these surfaces?
There are 3 types of heat transfer

- Conduction

- Convection

- Radiation

6.1   Conduction

Conduction is the transfer of energy from the more energetic particles of a substance to the adjacent less energetic ones as a result of interaction between particles.

$$\dot{Q}_{cond} = -kA\frac{\Delta T}{\Delta x} \tag{6.1}$$

In differential form

$$\dot{Q}_{cond} = -kA\frac{dT}{dx}$$

where k is the thermal conductivity of the material, which is a measure of the ability of a material to conduct heat. A is the area of the surface. ΔT is the temperature difference of the material and what it is in contact with. Δx is the thickness of the material.

6.2   Convection

Convection is the transfer of energy between a solid surface and the adjacent fluid that is in motion, and it involves the combined effects of conduction and fluid motion. The equation of convection is derived from Newtons law of cooling.

$$\dot{Q}_{conv} = hA_s(T_s - T_\infty) \tag{6.2}$$

31

where h is the convection heat transfer coefficient, A_s is the surface area. T_s is the surface temperature. T_∞ is the temperature of the fluid sufficiently far away from the surface. h is not a property of the fluid, but an experimental determined parameter whose value depends on all the variables influencing convection such as the surface geometry, the nature of fluid motion, the properties of the fluid and the bulk fluid velocity (Cengel et al., 2012).

6.3 Radiation

Radiation is the transfer of energy due to emission of electromagnetic waves (or photons). The heat transfer from convection dominates at low temperatures ($< 150 - 200°C$), but above $400°C$, radiation becomes increasingly dominant.

$$\dot{Q}_{rad} = \epsilon \sigma A_s (T_s^4 - T_{surr}^4) \tag{6.3}$$

where ϵ is the emissivity of the surface, $0 \leq \epsilon \leq 1$. A black body has an emissivity $\epsilon = 1$. σ is the Stefan-Boltzmann constant, $\sigma = 5.670 \cdot 10^{-8} \frac{W}{m^2 K^4}$. T_s is the surface temperature. T_{surr} is the temperature of the surrounding surfaces.

We will now demonstrate heat transfer with an example.
Consider steady heat transfer between two parallel plates, with an area of $A = 1m^2$, at constant temperatures of $T_1 = 500K$ and $T_2 = 300K$ that are $L = 10cm$ apart, see figure 9. Also, let us assume the plates are black, and therefore have an emissivity $\epsilon = 1$. The gap between the plates are filled with air. We then find the heat transfer between the two plates.
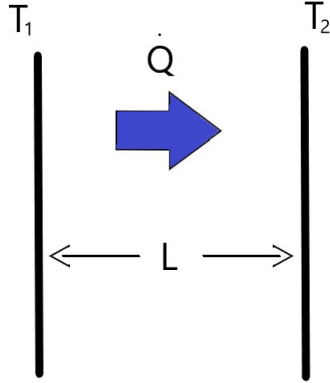
Figure 9: Heat transfer between two parallel plates

Assuming no convection currents in the air between the plates, the system will experience heat transfer due to conduction and radiation. Thus, equations 6.1 and 6.3 will be used for this example. The thermal conductivity of air at the average temperature of $400K$ is $k = 0.0326$, found by interpolating values from a table with properties of air at 1 atm pressure.

The rates of conduction and radiation heat transfer between the plates are

$$\dot{Q}_{cond} = -kA\frac{\Delta T}{\Delta x} = kA\frac{T_1 - T_2}{L}$$

$$\dot{Q}_{rad} = \epsilon\sigma A(T_1^4 - T_2^4)$$

By inserting the numbers given above, we find

$$\dot{Q}_{cond} = 65W$$

and

$$\dot{Q}_{rad} = 3084W$$

Therefore, the total heat transfer between the plates are

$$\dot{Q}_{total} = \dot{Q}_{cond} + \dot{Q}_{rad} = 3149W$$

Notice how large the contribution from radiation is compared to conduction. By deriving the ratio between radiation and conduction we get,

$$\frac{\dot{Q}_{rad}}{\dot{Q}_{cond}} = \frac{\epsilon\sigma L}{k}\left(T_1^3 + T_1 T_2^2 + T_2 T_1^2 + T_2^3\right) \tag{6.4}$$

For large temperatures, this ratio increases rapidly, which supports what we discussed in Section 6.3.

This example is a special case of heat transfer with nice and simple properties. In reality, this is much more involved.

6.4   Experimental research

An attempt of investigating instantaneous heat transfer in highly rated DI diesel engine by measuring key locations within the combustion chamber (valve bridge, above the piston bowl lip and bore edge) has been done by Jackson, Pilley and Owen (1990).
According to their report, the basic objectives of the experimental program were as follows:

- To define the spatial variation of instantaneous total and radiative heat transfer within the combustion chamber of a premium class, highly rated, heavy duty direct injection diesel engine.

- To further investigate the effect of wall temperature on instantaneous heat transfer in a thermally insulated version of the same engine.

Three heat flux probes were used in the experiment to measure radiative and conductive heat transfer.

The total heat flux probe was used to measure wall temperatures in combustion chambers. Due to wide variation in properties of materials may have caused inaccuracies in this type of measurement. However, Jackson et al. (1990) mention that the measurements have been reliable in previous experimental studies.

Radiative Probe was used to measure radiative heat transfer. Heat radiation in a firing engine occurs at light wavelengths well into the infrared. The probe were equipped with a sapphire window capable to transmit 85% up to a wavelength of five micrometer.

The experiment was conducted using a test engine with similar properties of a typical diesel engine. A series of tests with varying attributes, such as speed, torque and load, were used to provide different results based on these attributes.

With 1300rpm and 100% load, the peak heat transfer results were $175kW$ with a surface temperature of $650°C$.

As we discussed earlier, heat transfer from radiation becomes dominant for high temperatures, and is also shown in equation 6.4. The main issue of the experiments is that the emitted light from radiation has a wavelength up to five micrometers, and thus is not Planck distributed. Planck's law describes the spectral density of electromagnetic radiation emitted by a black body in thermal equilibrium at a given temperature T. The energy density is given by

$$u_\nu = \frac{8\pi h\nu}{c^3} \frac{1}{e^{h\nu/\sigma T} - 1} \tag{6.5}$$

where ν is the frequency of the emitted radiation, h and σ are Planck's and Boltzmann's constants, respectively. Energy of radiation is obtained by integrating over all frequencies. Since the experimental result only detects wavelengths up to 5 micrometers, the results will accordingly be inaccurate. Inaccuracies in a dominating heat transfer component will be crucial for the total heat transfer results.

7 Statistical model

This section is based on Dobson and Barnett (2008). The number of times an event occur inside a time interval is often modelled by a **Poisson distribution**. If Y is the number of events occurring in $[0, t]$, its probability distribution can be written as

$$f(y) = \frac{(\lambda t)^y}{y!} e^{-\lambda t}, \quad y = 0, 1, 2, ... \tag{7.1}$$

where $\mu = E(Y) = \lambda t$ is the expected number of occurrences. For a Poisson distribution, the variance is equal to the expected value, $\text{Var}(Y) = \lambda t$. The parameter λ represent the expected number of events per unit, and is called the intensity, or the rate of the process.

For fire in HGVs in tunnels, the rate parameter may be defined in many different ways, e.g fires per tunnel per year or fires per km of tunnel per year. More generally, the rate is specified in terms of units of exposure. Each HGV is exposed to the possibility of a fire in a tunnel once it enters the tunnel. Other variables such as the geometry of a given tunnel or the type of tunnel needs to be taken into account when modelling the rate of fire occurrences.

7.1 Poisson regression model

Poisson regression is used to model impact of explanatory variables on the rate of events. Let $Y_1, ..., Y_N$ be independent random variables with Y_i denoting the number of events observed from exposure t_i. The Poisson regression model, which is a special case of a generalized linear model, can be written as

$$E(Y_i) = \mu_i = t_i \lambda_i = t_i e^{\boldsymbol{x}_i \boldsymbol{\beta}}, \quad Y_i \sim Po(t_i \lambda_i) \tag{7.2}$$

where the term $\lambda_i = e^{\boldsymbol{x}_i \boldsymbol{\beta}}$ represent the explanatory variables affecting an event. The vectors $\boldsymbol{x}_i = [1, x_1, \ldots, x_k]_i$ and $\boldsymbol{\beta} = [\beta_0, \beta_1, \ldots, \beta_k]^T$ are covariates (variables affecting an event) and parameters (estimated in the model), respectively. A model with several exposure parameters will have an exposure parameter as a product of all exposure parameters $t_i = t_{1i} \cdot t_{2i} \cdots t_{ni}$. The natural link function is the logarithmic function

$$\log \mu_i = \log(t_i) + \boldsymbol{x_i} \boldsymbol{\beta} \tag{7.3}$$

where the term $\log(t_i)$ is called the **offset** and is a known constant.

Interpretation of regression coefficients

Let us consider that we have formulated a regression model, and we have found an expected number of events for a particular case. Now, we want to know what happens with the expected number of events if we increase a covariate by one unit, and let the other covariates remain constant. Let us assume the covariate of interest has some value $x_{ik} = a$, that can be found in our data. We use the natural link function found in equation 7.3

$$\log(E(Y_i \mid x_{ik} = a) = \log t_i + \sum_{j \neq k} x_{ij}\beta_j + x_{ik}\beta_k$$

$$= \log t_i + \sum_{j \neq k} x_{ij}\beta_j + a\beta_k$$

and calculate the difference of the link function before and after we increased the covariate by one unit.

$$\log(E(Y_i \mid x_{ik} = a + 1) - \log(E(Y_i \mid x_{ik} = a) \tag{7.4}$$

$$= \log t_i + \sum_{j \neq k} x_{ij}\beta_j + (a + 1)\beta_k - \left(\log t_i + \sum_{j \neq k} x_{ij}\beta_j + a\beta_k \right)$$

$$= \beta_k$$

We exponentiate both sides and obtain

$$RR_k = \frac{E(Y_i \mid x_{ik} = a + 1)}{E(Y_i \mid x_{ik} = a)} = e^{\beta_k} \tag{7.5}$$

which is often called the **rate ratio**.

Thus, increasing x_{ik} by one unit will result in a multiplicative effect of e^{β_k} on the rate μ.

$$E(Y_i \mid x_{ik} = a + 1) = e^{\beta_k} E(Y_i \mid x_{ik} = a) \tag{7.6}$$

More generally, increasing x_{ik} by c units, will result in a multiplicative effect of $e^{c\beta_k}$ on the rate μ

$$E(Y_i \mid x_{ik} = a + c) = e^{c\beta_k} E(Y_i \mid x_{ik} = a) \tag{7.7}$$

Estimating the parameters

Parameters β_k will be estimated by maximum likelihood estimation (MLE). Wald statistics are used for performing hypothesis tests and calculating estimates of confidence intervals. A Poisson regression model has a probability density function

$$f(y_i; \lambda_i) = \frac{(t_i \lambda_i)^{y_i} e^{-t_i \lambda_i}}{y_i!} \tag{7.8}$$

where $\lambda_i = e^{\boldsymbol{x}_i \boldsymbol{\beta}}$. Equation 7.8 can be written as

$$f(y_i; \lambda_i) = e^{y_i \boldsymbol{x}_i \boldsymbol{\beta} - t_i e^{\boldsymbol{x}_i \boldsymbol{\beta}} + y_i \ln(t_i) - \ln(y_i!)} \tag{7.9}$$

which means that the probability density function is of the canonical exponential family form (Dobson and Barnett, 2008). Furthermore, the likelihood function is

$$L(\boldsymbol{\beta}) = \prod_{i=1}^{n} e^{y_i \boldsymbol{x}_i \boldsymbol{\beta} - t_i e^{\boldsymbol{x}_i \boldsymbol{\beta}} + y_i \ln(t_i) - \ln(y_i!)}$$

$$L(\boldsymbol{\beta}) = \exp\left(\sum_{i=1}^{n} \left[y_i \boldsymbol{x}_i \boldsymbol{\beta} - t_i e^{\boldsymbol{x}_i \boldsymbol{\beta}} + y_i \ln(t_i) - \ln(y_i!) \right] \right) \tag{7.10}$$

It is easier to work with the log-likelihood function

$$l(\boldsymbol{\beta}) = \log(L(\boldsymbol{\beta})) = \sum_{i=1}^{n} \left[y_i \boldsymbol{x}_i \boldsymbol{\beta} - t_i e^{\boldsymbol{x}_i \boldsymbol{\beta}} + y_i \ln(t_i) - \ln(y_i!) \right] \tag{7.11}$$

The maximum likelihood estimator (MLE) is defined as

$$\hat{\boldsymbol{\beta}} = \underset{\beta}{\operatorname{argmax}}\ l(\boldsymbol{\beta}) \tag{7.12}$$

i.e the values $\boldsymbol{\beta}$ that maximize the log-likelihood function. We can find maxima of a function by differentiating and finding values for $\boldsymbol{\beta}$ such that the derivatives equal zero.

$$\frac{\partial l(\boldsymbol{\beta})}{\partial \boldsymbol{\beta}} = 0$$

$$\frac{\partial}{\partial \boldsymbol{\beta}}\left(\sum_{i=1}^{n} \left[y_i \boldsymbol{x}_i \boldsymbol{\beta} - t_i e^{\boldsymbol{x}_i \boldsymbol{\beta}} + y_i \ln(t_i) - \ln(y_i!) \right] \right) = 0 \tag{7.13}$$

For the special case when β is a scalar, we have

$$\frac{\partial}{\partial \beta}\left(\sum_{i=1}^{n} \left[y_i x_i \beta - t_i e^{x_i \beta} + y_i \ln(t_i) - \ln(y_i!) \right] \right) = 0$$

$$\sum_{i=1}^{n} x_i(y_i - t_i e^{x_i \beta}) = 0 \tag{7.14}$$

Equation 7.14 can not be solved analytically. However, we can approximate $\hat{\beta}$ iteratively by numerical methods. Also, the second derivative test is used to check if the critical values of β is a maximum or a minimum.

$$\frac{\partial^2 l(\beta)}{\partial \beta^2} = -\sum_{i=1}^{n} t_i x_i^2 e^{x_i \beta} < 0 \tag{7.15}$$

Since $t_i > 0$, and of course $x_i^2 > 0$ and $e^{x_i \beta} > 0$, the second derivative is negative everywhere, and $l(\beta)$ is globally concave down. Thus, equation 7.14 has a unique critical point $\hat{\beta}$ which maximizes $l(\beta)$.

More generally, the score vector is used to estimate all values of the parameter vector $\boldsymbol{\beta}$. The score vector is derived from the MLE-method and is defined as

$$U(\boldsymbol{\beta}) = \nabla l(\boldsymbol{\beta}) = \left[\frac{\partial l(\boldsymbol{\beta})}{\partial \beta_0}, \frac{\partial l(\boldsymbol{\beta})}{\partial \beta_1}, ..., \frac{\partial l(\boldsymbol{\beta})}{\partial \beta_k}\right]^T \tag{7.16}$$

Solve $U(\boldsymbol{\beta}) = \mathbf{0}$ by numerical methods to obtain $\hat{\boldsymbol{\beta}}$.

The covariance of the score vector is known as the Fisher information matrix

$$Cov(U(\boldsymbol{\beta})) = E[U_j(\boldsymbol{\beta})U_k(\boldsymbol{\beta})] = -E\left[\nabla^2 l(\boldsymbol{\beta})\right] = \mathcal{J}(\boldsymbol{\beta}) \tag{7.17}$$

$$\mathcal{J}(\boldsymbol{\beta}) = -E \begin{bmatrix} \frac{\partial^2 l(\boldsymbol{\beta})}{\partial \beta_0^2} & \frac{\partial^2 l(\boldsymbol{\beta})}{\partial \beta_0 \beta_1} & \cdots \\ \frac{\partial^2 l(\boldsymbol{\beta})}{\partial \beta_0 \beta_1} & \frac{\partial^2 l(\boldsymbol{\beta})}{\partial \beta_1^2} & \cdots \\ \vdots & \vdots & \ddots \end{bmatrix} \tag{7.18}$$

The fisher information matrix can be used to estimate the standard deviation of $\hat{\beta}_i$. The estimated standard deviation for $\hat{\beta}_i$ are found as the square root of the i'th diagonal element of the inverse information matrix, $\mathcal{J}^{-1}$ (Dobson and Barnett, 2008).

$$SD(\hat{\beta}_i) = \sqrt{\mathcal{J}_{ii}^{-1}(\boldsymbol{\beta})} \tag{7.19}$$

7.2 Confidence interval and p-value

Confidence interval

The sampling distribution of the MLE when $f(y_i; \lambda_i)$ is the true model, is asymptotically normal (Kleppe, 2015). This is an important result because we can treat the Poisson regression model as any statistical model. In particular we can use MLE theory to perform hypothesis tests and find confidence intervals. The Wald confidence interval are found by using the results from equations 7.16 and 7.19

$$(\hat{\beta}_k \pm z_{\alpha/2} SD(\hat{\beta}_k)) \tag{7.20}$$

The value of $z_{\alpha/2}$ can be found in a z-table, with a respective confidence interval. It is conventional to choose a 95% confidence interval, where $z_{0.025} = 1.96$.

Hypothesis testing

Hypothesis testing is used to determine whether a null hypothesis can be rejected in favour of an alternative hypothesis. We need to formulate a null hypothesis and an alternative hypothesis based on our model. For the case of testing parameters β_k, a null hypothesis could be that covariate k does not have any influence

$$H_0 : \beta_k = 0$$

An alternative hypothesis could be that the expected number of accidents are actually influenced by covariate k

$$H_a : \beta_k \neq 0$$

Since parameter estimators, $\hat{\beta}_k$, obtained by maximum likelihood are approximately normally distributed (Kleppe, 2015)

$$\frac{\hat{\beta}_k - \beta_k}{s.e.(\hat{\beta}_k)} \sim \mathrm{N}(0, 1) \tag{7.21}$$

Applying the null hypothesis to equation 7.21, we can find a value for the test statistics under the null-hypothesis that $\beta_k = 0$.

$$z_{obs} = \frac{\hat{\beta}_k}{s.e(\beta_k)}$$

We reject the null hypothesis if the value of the test statistic is very unlikely under the null hypothesis, more precisely if $|z_{obs}| > z_{\alpha/2}$. α is the significance level of the test, and it is conventional to choose $\alpha = 0.05$.

A **p-value** is the probability of observing at least as extreme data as observed given that the null hypothesis is correct. The null hypothesis in our case is that the number of accidents are not influenced by covariate k. Under the null hypothesis we calculate how likely it is to get a value of $\hat{\beta}_k$ deviating at least as much from 0 as what we observed. This is done by calculating the p-value

$$\text{p-value} = 2 \cdot P(z \leq -|z_{obs}|) \tag{7.22}$$

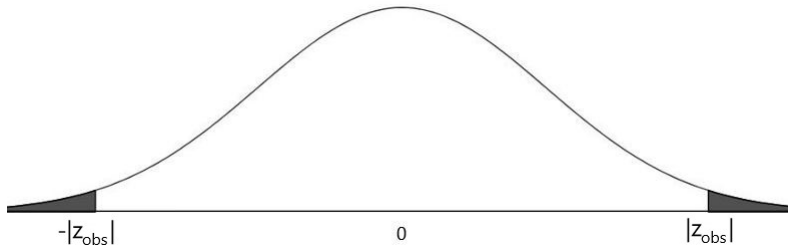We get a factor of 2 because of the two-tailed test, see figure 10.

Figure 10: Normal distribution

A variable is significant under the model if it has a low p-value. We reject the nullhypothesis when p-value $\leq \alpha$. Significant means that there is a real statistical relationship. Variables that are not significant, can be removed without affecting the model. We will see later how we can eliminate insignificant variables until the model contains nothing but significant variables.

A related way of deciding whether covariate k influences the expected number of fire accidents is by considering the confidence interval. If the resulting confidence interval from equation 7.20 does not contain $\beta_k = 0$, it implies that covariate k influence the expected number of accidents. If the entire confidence interval is greater than 0, it implies that increasing values of covariate k truly increase the expected number of accidents. Similarly, if the entire confidence interval is less than 0, it implies that increasing values of covariate k truly decrease the expected number of accidents.

7.3   Example

We will now demonstrate the theory of Poisson regression for an example with only one covariate.

Let $\boldsymbol{\beta} = [\beta_0, \beta_1]$ and $x_0 = 1$ such that the rate $\lambda_i = e^{\beta_0 + x_i \beta_1}$, where β_0 is called the intercept of the model. Then, equations 7.16 and 7.18 becomes

$$U(\boldsymbol{\beta}) = \begin{bmatrix} \sum_{i=1}^{n} y_i - t_i \lambda_i \\ \sum_{i=1}^{n} x_i (y_i - t_i \lambda_i) \end{bmatrix}$$

and

$$\mathcal{J}(\boldsymbol{\beta}) = -E \begin{bmatrix} -\sum_{i=1}^{n} t_i \lambda_i & -\sum_{i=1}^{n} x_i t_i \lambda_i \\ -\sum_{i=1}^{n} x_i t_i \lambda_i & -\sum_{i=1}^{n} x_i^2 t_i \lambda_i \end{bmatrix}$$

$$= \begin{bmatrix} \sum_{i=1}^{n} t_i \lambda_i & \sum_{i=1}^{n} x_i t_i \lambda_i \\ \sum_{i=1}^{n} x_i t_i \lambda_i & \sum_{i=1}^{n} x_i^2 t_i \lambda_i \end{bmatrix}$$

The estimates for $\hat{\boldsymbol{\beta}}$ are found numerically by solving $U(\boldsymbol{\beta}) = \mathbf{0}$. The estimated standard deviation for $\hat{\beta}_i$ are found using equation 7.19

Recall that for a $2x2$ matrix

$$A = \begin{bmatrix} a & b \\ c & d \end{bmatrix}$$

the formula for its inverse is

$$A^{-1} = \frac{1}{ad - bc} \begin{bmatrix} d & -b \\ -c & a \end{bmatrix}$$

The inverse information matrix can be written as

$$\mathcal{J}^{-1} = \frac{1}{\sum_{i=1}^{n} t_i \lambda_i \sum_{i=1}^{n} x_i^2 t_i \lambda_i - \sum_{i=1}^{n} x_i t_i \lambda_i \sum_{i=1}^{n} x_i t_i \lambda_i} \begin{bmatrix} \sum_{i=1}^{n} x_i^2 t_i \lambda_i & -\sum_{i=1}^{n} x_i t_i \lambda_i \\ -\sum_{i=1}^{n} x_i t_i \lambda_i & \sum_{i=1}^{n} t_i \lambda_i \end{bmatrix}$$
$$(7.23)$$

By substituting equation 7.23 into equation 7.19, we can find the standard deviation for $\hat{\beta}_1$

$$SD(\hat{\beta}_1) = \sqrt{\frac{\sum_{i=1}^{n} t_i \lambda_i}{\sum_{i=1}^{n} x_i^2 t_i \lambda_i \sum_{i=1}^{n} t_i \lambda_i - \sum_{i=1}^{n} x_i t_i \lambda_i \sum_{i=1}^{n} x_i t_i \lambda_i}} \qquad (7.24)$$

Suppose we wish to estimate parameters of subsea tunnels. By conducting a univariate model, see table 4, we find the parameter for the covariate "subsea" to be $\hat{\beta}_1 = 2.34$. Subsea tunnels have $x = 1$ and non-subsea tunnels have $x = 0$. We can find the standard deviation of $\hat{\beta}_1$ by using equation 7.24 with $\sum_{i=1}^{n} t_i \lambda_i = 131$ and $\sum_{i=1}^{n} x_i t_i \lambda_i = \sum_{i=1}^{n} x_i^2 t_i \lambda_i = 53$.

$$SD(\hat{\beta}_1) = \sqrt{\frac{131}{131 \cdot 53 - 53 \cdot 53}} = 0.178$$

We then get the 95% Wald confidence interval for β_1

$$(\hat{\beta}_1 \pm 1.96 SD(\hat{\beta}_1)) = 2.34 \pm 1.96 \cdot 0.178 = (2.0, 2.7)$$

An associated p-value is found using equation 7.22

$$\text{p-value} = 2P(z \leq -13.167) = 1.36 \cdot 10^{-39}$$

where we have used the "pnorm()" function in R to calculate $P(z \leq -13.167)$. And so we are very certain the subsea tunnels affect the number of fire occurrences in heavy goods vehicles in Norwegian road tunnels.

Alternatively, this conclusion could be drawn straight from the confidence interval. Since the interval does not cross 0, it indicates that subsea tunnels truly increase the number of incidents over time. The Wald confidence interval can also be used to find the confidence interval for the rate ratio. In this case, the 95% confidence interval for RR is

$$e^{(\hat{\beta}_1 \pm 1.96 SD(\hat{\beta}_1))} = (7.3, 14.8)$$

Similarly, since the interval does not cross 1, subsea tunnels truly increase the number of incidents.

7.4 Goodness of fit

Testing the goodness of fit for a particular model is done by calculating residuals. Residuals tell how far off the estimated values are from the observation. There are several types of residuals, but we focus on these two: Pearson residuals and deviance residuals.

The **Pearson residuals** are the difference in the observed and estimated values, divided by the standard error of the estimates. Since $\text{Var}(Y_i) = E(Y_i)$ for a Poisson distribution, the standard error is the square root of the estimated expectation.

$$r_i = \frac{Y_i - t_i \hat{\lambda}_i}{\sqrt{t_i \hat{\lambda}_i}} = \frac{Y_i - \hat{\mu}_i}{\sqrt{\hat{\mu}_i}} \tag{7.25}$$

where Y_i are the observed values, and $\hat{\mu}_i$ are the estimated values of $E(Y_i)$. Ideally, we want to have $\hat{\mu}_i$ close to Y_i and randomly fluctuating around Y_i. Cases with $r_i > 0$ have more observed than expected number of events, and cases with $r_i < 0$ have less observed than expected number of events. For the

Poisson distribution, the residuals given in equation 7.25 and the chi-squared goodness of fit statistics are related by (Dobson and Barnett, 2008)

$$X^2 = \sum r_i^2 = \sum \frac{(Y_i - \hat{\mu}_i)^2}{\hat{\mu}_i} \qquad (7.26)$$

In practice, we use the standardized Pearson residuals

$$r_i = \frac{Y_i - \hat{\mu}_i}{\sqrt{\hat{\mu}_i}\sqrt{1 - h_{ii}}} \qquad (7.27)$$

where h_{ii} is the ith element of the hat matrix, $\boldsymbol{H} = \boldsymbol{X}(\boldsymbol{X}^T\boldsymbol{X})^{-1}\boldsymbol{X}^T$, also known as the **leverage** of the ith observation (Dobson and Barnett, 2008). $\boldsymbol{X}$ is the matrix of all covariate vectors $\boldsymbol{x}_i$,

$$\boldsymbol{X} = \begin{bmatrix} \boldsymbol{x}_1 \\ \vdots \\ \boldsymbol{x}_N \end{bmatrix}$$

A high leverage indicates that the ith observation is influential, and may be a concern. We will later discuss how we can capture these influential observations and how we can treat them in the model.

In R, standardized Pearson residuals are computed without the ith observations, $(Y_i, \boldsymbol{x}_i)$. R runs the regression model without using observation i. Then

$$r_i = \frac{Y_i - t_i\hat{\lambda}_i}{\sqrt{t_i\hat{\lambda}_i}}$$

where $\hat{\lambda}_i = e^{\boldsymbol{x}_i\hat{\boldsymbol{\beta}}^{(-i)}}$ and $\hat{\boldsymbol{\beta}}^{(-i)}$ is the estimate of $\boldsymbol{\beta}$ without observation i. The omitted observation, Y_i, is then compared with the expected value $\hat{\mu}_i = t_i\hat{\lambda}_i = t_i e^{\boldsymbol{x}_i\hat{\boldsymbol{\beta}}^{(-i)}}$. By computing the standardized Pearson residuals without the ith observation leads to an independency between the numerator and denominator in equation 7.27. Because the model exclude the ith observation, the residuals are also called standardized deletion residuals (R-Forge, 2019)

Pearson residuals are used to verify whether or not the Poisson regression model is a good model for a particular case. This can be done by plotting the residuals versus $\boldsymbol{x}_i\hat{\boldsymbol{\beta}}$, and look for patterns. One can also plot the residuals against each variable, x_{ij}. Figure 11 is a typical pattern for a good fit.

The string of points shaped like a tail, are points usually with zero observed events. Thus, $r_i = -\sqrt{\hat{\mu}_i}$, which explains the shape of the tail. Also, there are 2 points far away from the tail. They are called outliers, and we may consider performing the analysis without these observation to determine how this impact the result (Minitab support team, 2019), see Section 8.2 Poisson regression model 1. Alternatively, we can see if we can change the model to better fit these data points.
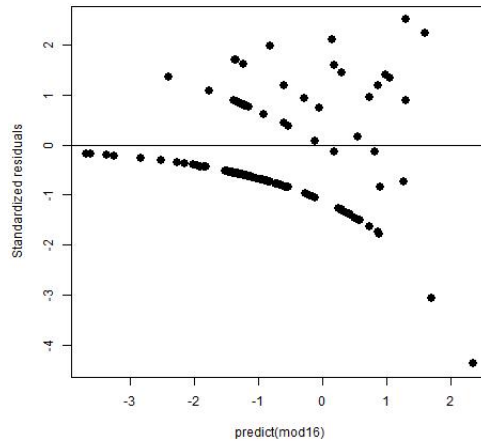

Figure 11: Plot of standardized deletion residuals vs. $\boldsymbol{x}_i\boldsymbol{\beta}$

Deviance residuals
The deviance, also called the **log-likelihood (ratio) statistics** are used similarly to Pearson to test the goodness of fit of the model.
Let $\hat{\boldsymbol{\beta}}_{(max)}$ denote a saturated model where there are n parameters such that $\hat{\mu}_{i,max} = t_i\hat{\lambda}_{i,max} = Y_i$, and let $\hat{\boldsymbol{\beta}}$ denote the fitted model where $\hat{\mu}_i = t_i\hat{\lambda}_i$. The log-likelihood function from equation 7.11 can be written as follows

$$l(\boldsymbol{\beta}) = \sum_{i=1}^{n}[Y_i\ln(t_i\hat{\lambda}_i) - \ln(Y_i!) - t_i\hat{\lambda}_i] = \sum_{i=1}^{n}[Y_i\ln(\hat{\mu}_i) - \ln(Y_i!) - \hat{\mu}_i] \quad (7.28)$$

We can then find the **deviance** of the model

$$D = 2\{l(\hat{\boldsymbol{\beta}}_{(max)}) - l(\hat{\boldsymbol{\beta}})\} = 2\left\{\sum_{i=1}^{n}[Y_i\ln(Y_i) - \ln(Y_i!) - Y_i] - \sum_{i=1}^{n}[Y_i\ln(\hat{\mu}_i) - \ln(Y_i!) - \hat{\mu}_i]\right\}$$

$$D = 2 \sum_{i=1}^{n} [Y_i \ln(\frac{Y_i}{\hat{\mu}_i}) - (Y_i - \hat{\mu}_i)] \qquad (7.29)$$

From this we get the **deviance residuals**

$$d_i = \text{sign}(Y_i - \hat{\mu}_i)\sqrt{2[Y_i \ln(\frac{Y_i}{\hat{\mu}_i}) - (Y_i - \hat{\mu}_i)]} \qquad (7.30)$$

The Pearson and deviance residuals are approximately equal. This can be shown by using Taylor series expansion of $f(Y_i) = Y_i \ln \left(\frac{Y_i}{\hat{\mu}_i}\right)$ about $Y_i = \hat{\mu}_i$.

$$f(Y_i) = f(\hat{\mu}_i) + f'(\hat{\mu}_i)(Y_i - \hat{\mu}_i) + \frac{1}{2}f''(\hat{\mu}_i)(Y_i - \hat{\mu}_i)^2 + ...$$

$$f(Y_i) = 0 + 1(Y_i - \hat{\mu}_i) + \frac{1}{2}\frac{1}{\hat{\mu}_i}(Y_i - \hat{\mu}_i)^2 + ...$$

so,

$$Y_i \ln \left(\frac{Y_i}{\hat{\mu}_i}\right) \simeq (Y_i - \hat{\mu}_i) + \frac{1}{2}\frac{(Y_i - \hat{\mu}_i)^2}{\hat{\mu}_i} \qquad (7.31)$$

Substituting this in to equation 7.29, we obtain

$$D = 2 \sum_{i=1}^{n} \left[(Y_i - \hat{\mu}_i) + \frac{1}{2}\frac{(Y_i - \hat{\mu}_i)^2}{\hat{\mu}_i} - (Y_i - \hat{\mu}_i) \right]$$

$$= \sum_{i=1}^{n} \frac{(Y_i - \hat{\mu}_i)^2}{\hat{\mu}_i} = X^2$$

In addition to residuals, there are numerous other methods to assess the adequacy of a model and to identify unusual or influential observations. **Cooks distance** is a measurement which combine standardized residuals and leverage

$$D_i = \frac{1}{p}\left(\frac{h_{ii}}{1 - h_{ii}}\right)r_i^2 \qquad (7.32)$$

where p is the number of parameters (Dobson and Barnett, 2008). Cooks distance, D_i, measures how much influence each observation has for the estimated values of the model. Large values of Cooks distance may indicate that the ith observation is influential. A general rule of thumb; Cooks distance greater than unity may require further investigation (Dobson and Barnett, 2008). One should also investigate any values that sticks out from the others. We can plot Cooks distance vs. observation number so that we can detect influential observations. This is shown in figure 16.

Akaike information criterion

Akaike information criterion (AIC) is a function of log-likelihood and the number of parameters in the fitted model

$$AIC = -2l(\hat{\boldsymbol{\beta}}) + 2p \qquad (7.33)$$

where p is the number of parameters in the fitted model.

We may compare models based on their AIC values. When comparing models fitted by maximum likelihood to the same data, the smaller the AIC, the better the fit (Dobson and Barnett, 2008).

8 Regression model for fire occurrences in heavy goods vehicles in road tunnels

In this section we will apply the Poisson regression model discussed in Section 7 to our data. Our goal is to estimate the expected number of developing and fully developed fire incidents in HGVs due to technical failures in road tunnels. We will also try to make a reasonable conclusion of which variables are most influential and how these variables influence the expected number of incidents.

8.1 Collection of data

Source of data:

- Road tunnels and road tunnels geometry from the NPRA

- Roadmap (Vegkart) (Statens vegvesen, 2019)

- Data of road tunnel fire incidents from 2001-2015 (Nævestad, 2016)

The data has been accumulated such that every road tunnel in Norway longer than 500 m is included (except a few due to missing data). An Excel sheet of road tunnels and road tunnels geometry has been provided by the NPRA. It was the starting point used to sort and collect data on each tunnel, and also to gather information about the tunnels. In total 485 unique tunnels have been used out of the 538 tunnels in Norway longer 500 meter (there are totally 1202 Norwegian tunnels).

For each tunnel we have gathered data of 11 different variables. These are variables that we expect will influence fire accidents in road tunnels, and also variables that are measurable and can be collected from some source. These variables are (each of the variables are explained below);

- Fire incidents

- Number of years with data

- Length

- Slope

- Slope downward

- Length downward

- Slope upward

- Length upward

- Annual average daily traffic (AADT)

- Annual average daily traffic for heavy goods vehicles (AADT HGV)

- Subsea

Fire incidents, or more specifically, developing or fully developed fires in HGV in tunnels due to technical failure is our response variable. We wish to model which factors influence the number of fire incidents. We have used Nævestads data of incidents that has been collected from the years 2001-2015, see table 3. Developing fire are also denoted near fires, and the criteria of its recordings is questionable, but we use TØIs recordings.

Number of years with data is an exposure parameter, t_i, for both modelling approaches, see Section 8.2 and Section 8.3. Since the data of accidents ranges from 2001-2015, the number of years with data has a maximum of 15 years, depending on whether or not a specific tunnel has been in operation all these years. If a tunnel was opened in 2011, it has only been exposed to accidents for 5 years.

The variable "length" is the length of each tunnel. In Section 8.3 length will be used as an exposure parameter instead of a covariate when we try to model accidents per length unit rather than per tunnel.

Length downward and upward are measurements of how far into the tunnel the incline descend or ascend. Since downward and upward lengths are relative to the direction of the vehicle entering a tunnel, we do not know what is up and what is down. We have therefore chosen each tunnel with the longest length up or down to be length up, and the shortest to be length down.
Slope is a variable representing the maximum slope of a tunnel. Slope downward and upward are average slopes downward and upward, respectively.
The NPRA data of tunnel geometry has been used for both slopes and lengths.

Annual average daily traffic (AADT) is a measurement of how many vehicles drive through a tunnel, on average, each day. The NPRA's roadmap (Statens vegvesen, 2019) has been used to collect data of AADT and AADT

49

for heavy goods vehicles. The roadmap does only show AADT for 2017. If AADT is changing each year, which presumably it does, the fact that NPRAs roadmap only gives AADT for 2017 may cause an inaccuracy for our studies. Thankfully, a recent study by TØI (Høye, Nævestad and Ævarsson, 2019), tackles this problem by presenting AADT development for private and freight transport in Norway from 2005 to 2017.
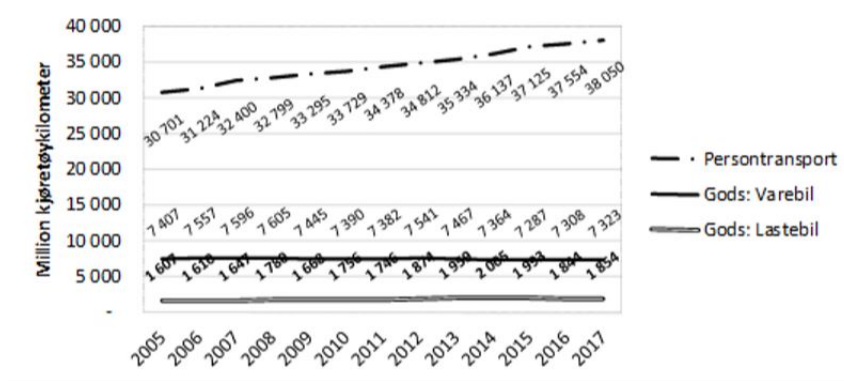

Figure 12: AADT development for personal and freight transport in Norway from 2005 to 2017, Høye et al. (2019)
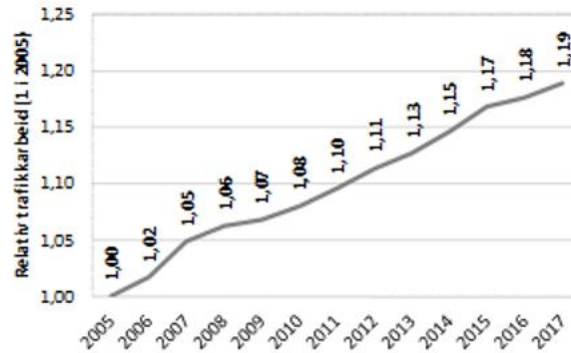
Figure 13: Relative traffic work from 2005 to 2017, Høye et al. (2019)

The relative traffic work is the relation between the developments in private transport vs. freight transport. Note from figure 12 that private transport seems to increase steadily. In fact, personal transport increase approximately linearly. By using this linearity, we can conclude that the average AADT of personal transport from 2001 to 2015 is approximately equal to

50

the median AADT for these years, i.e AADT in 2008. So, the average total AADT is equal to the AADT for 2017 multiplied by a factor of 1.06/1.19, see figure 13. Annual average daily traffic for heavy goods vehicles is assumed to be approximately unchanged over time, and we will therefore use the 2017 AADT found in the NPRA's roadmap.

Subsea is a variable that indicates whether a tunnel is subsea or not. If a tunnel is subsea, it gets a value of 1 and 0 otherwise. Subsea tunnels are particularly interesting as they tend to have an extreme geometry.

8.2 Poisson regression model 1

In the first model, we are going to estimate accidents per tunnel using the covariates described in section 8.1, with "Number of years with data" as an exposure parameter.

$$E(Y_i) = t_i\lambda_i = N_i\lambda_i$$

where N_i is the number of years with data for each tunnel.

Then for a given tunnel, λ_i models the expected number of accidents in tunnel i per 15 years, i.e $t = 1$ corresponds to 15 years. We will start off by estimating each covariate separately.

Variable	$\hat{\beta}$	p-value	Rate ratio	95% confidence interval
Slope	0.27	< 0.0001	1.31	1.20, 1.42
Length[km]	0.17	< 0.0001	1.18	1.13, 1.23
Subsea	2.34	< 0.0001	10.42	5.66, 19.18
AADT[1000]	0.05	< 0.0001	1.05	1.03, 1.08
AADT HGV[1000]	0.43	< 0.0001	1.54	1.32, 1.80
Slope downward	0.31	< 0.0001	1.36	1.26, 1.46
Length downward[km]	0.33	< 0.0001	1.39	1.26, 1.52
Slope upward	0.26	< 0.0001	1.30	1.17, 1.44
Length upward[km]	0.27	< 0.0001	1.31	1.20, 1.44

Table 4: Each variable estimated separately.
Number of observations: 485; offset: Number of years with data.

Note that all covariates have a confidence interval of the rate ratio with a lower bound larger than 1, indicating that each covariate truly increase the frequency of accidents.

The effect of subsea tunnels is very high compared to other covariates. This is because 11 out of 31 (36%) subsea tunnels have had at least one accident from 2001 to 2015, and 53 out of the total 131 (40%) accidents occurred in a subsea tunnel, while only 31 out of 485 (6%) of the tunnels are subsea. Next, we will estimate parameters using a model with all covariates simultaneously. The results are given in table 5.

Variable	$\hat{\beta}$	p-value	Rate ratio	95% confidence interval
Slope	-0.05	0.6305	0.95	0.77, 1.17
Length[km]	0.51	0.0303	1.67	1.05, 2.65
Subsea	1.37	0.0133	3.95	1.34, 11.69
AADT[1000]	0.003	0.9219	1.00	0.94, 1.07
AADT HGV[1000]	0.58	0.0166	1.79	1.11, 2.87
Slope downward	0.11	0.1496	1.12	0.96, 1.30
Length downward[km]	-0.55	0.0229	0.58	0.36, 0.93
Slope upward	0.20	0.0746	1.22	0.98, 1.52
Length upward[km]	-0.15	0.5474	0.86	0.53, 1.40

Table 5: All variables estimated simultaneously.
Number of observations: 485; offset: Number of years with data.
$AIC = 483.72$

Notice that none of the covariates are particularly significant. Because some variables are very similar, they tend to cancel each other out in the model, making the other insignificant.

Since Length = Length downward + Length upward, length down and up differs from length only by a factor of α_i and $(1 - \alpha_i)$, respectively. Also, length downward and upward does not contribute extra information to the model.

If, however, we wanted to estimate accidents on the way up or down a tunnel, given that we have data to support this, then length upward or downward would contribute extra information to the model.

Figure 14 shows how similar length is compared to length up and down, and equal when they are combined.
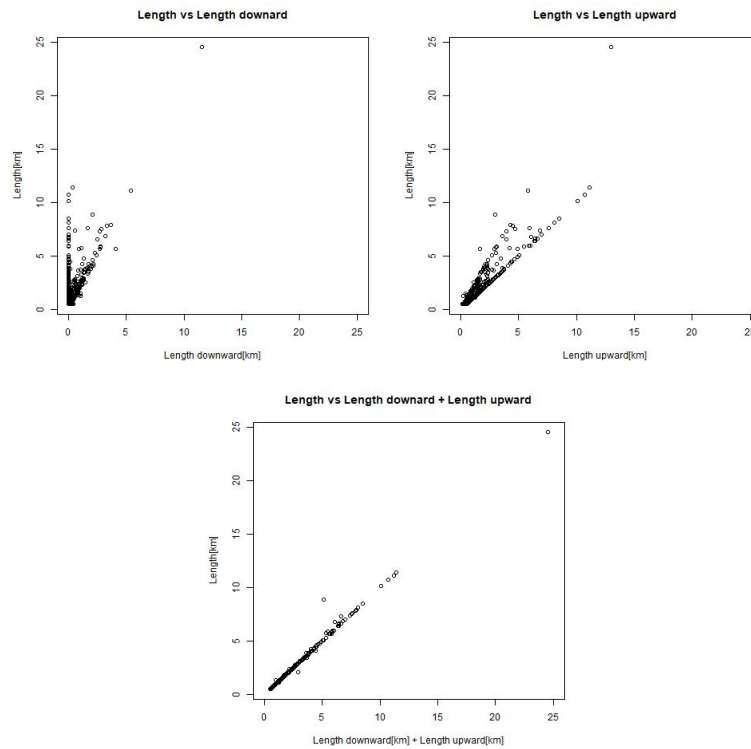
Figure 14: Plots of length against length downward, length upward and length downward + upward, respectively

As discussed in Section 7.2, we should remove insignificant variables. We will start by eliminating the least significant variable, AADT[1000]. Then, run the model again to see which variable becomes least significant, and remove it. Continue this process until we end up with only significant variables. The results are given in table 6.

Variable	$\hat{\beta}$	p-value	Rate ratio	95% confidence interval
(Intercept)	-3.16	< 0.0001	-	-
Slope	0.12	0.0069	1.13	1.03, 1.23
Length[km]	0.19	< 0.0001	1.20	1.17, 1.24
AADT HGV[1000]	0.57	< 0.0001	1.77	1.62, 1.94
Subsea	1.74	< 0.0001	5.72	3.04, 10.76

Table 6: Excluded insignificant variables from table 5.
Number of observations: 485; offset: Number of years with data.
$AIC = 494.99$

As discussed in Section 7.4, we may consider performing the analysis without observations that are considered outliers. By analysing the model from table 6, we find two influential observations, see figure 15. Two points are marked with a red circle. The points represent the Lærdal tunnel and the Vålerenga tunnel. Both the Lærdal tunnel and the Vålerenga tunnel have had 2 accidents in 15 years. Since the Lærdal tunnel is extremely long compared to other tunnels, it will get a large predicted number of accidents relative to its observed accidents. This explains why the residual $|r_i| >> 0$. Similarly, the Vålerenga tunnel has a high number of annual average daily traffic compared to other tunnels giving it a large predicted number of accidents. However, the Vålerenga tunnel is not as influential as the Lærdal tunnel.
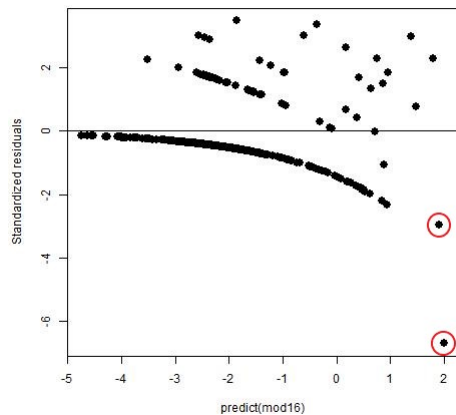

Figure 15: Plot of standardized deletion residuals vs. $\boldsymbol{x}_i\hat{\boldsymbol{\beta}}$.
The Lærdal tunnel and the Vålerenga tunnel are marked with red circles.

Recall that we can also plot Cooks distance versus observation number to detect influential observations. From figure 16, we see that the Lærdal tunnel is extremely influential. Although the Vålerenga tunnel seems to be okay in this plot, its Cooks distance $D_i > 1$, and may be influential.
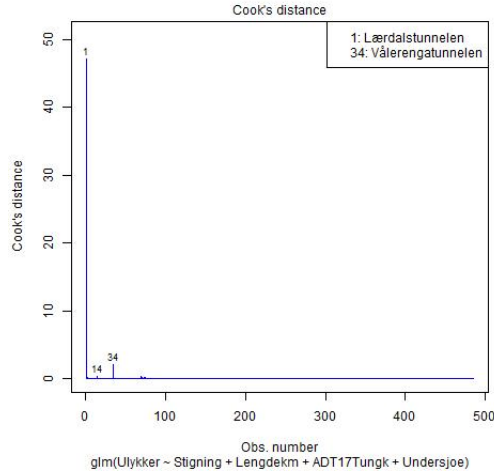

Figure 16: Cooks distance vs. observation number

These two plots give us a good indication to eliminate the Lærdal and Vålerenga tunnel from the model found in table 6. By doing this we get the following results

Variable	$\hat{\beta}$	p-value	Rate ratio	95% confidence interval
(Intercept)	-3.61	< 0.0001	-	-
Slope	0.14	0.0017	1.15	1.05, 1.25
Length[km]	0.34	< 0.0001	1.41	1.32, 1.50
AADT HGV[1000]	0.63	< 0.0001	1.89	1.70, 2.09
Subsea	1.22	< 0.0001	3.38	1.81, 6.30

Table 7: Excluded the Lærdal and the Vålerenga tunnel from the model in table 6.
Number of observations: 483; offset: Number of years with data.
$AIC = 455.33$

Note how this affect both the effect of length and the effect of annual average daily traffic. The effect of length has almost been doubled. Lærdal tunnel

55

is so long and with so few incidents, it "pushes" the slope of the line down. This phenomenon can be visualized in figure 17.

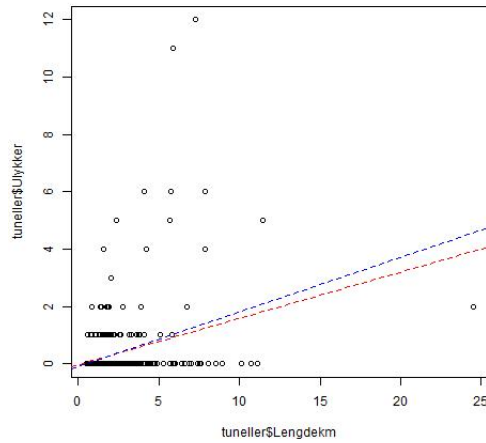Figure 17: Linear slope with (red) and without (blue) Lærdal tunnel

Although the residuals are not perfect, they behave much better now without these outliers. We have that tail, which we discussed in Section 7.4 below the zero-line that represent mostly tunnels without accidents. Points above the zero-line are tunnels with accidents and they are more spread due to variation of observed and predicted accidents.
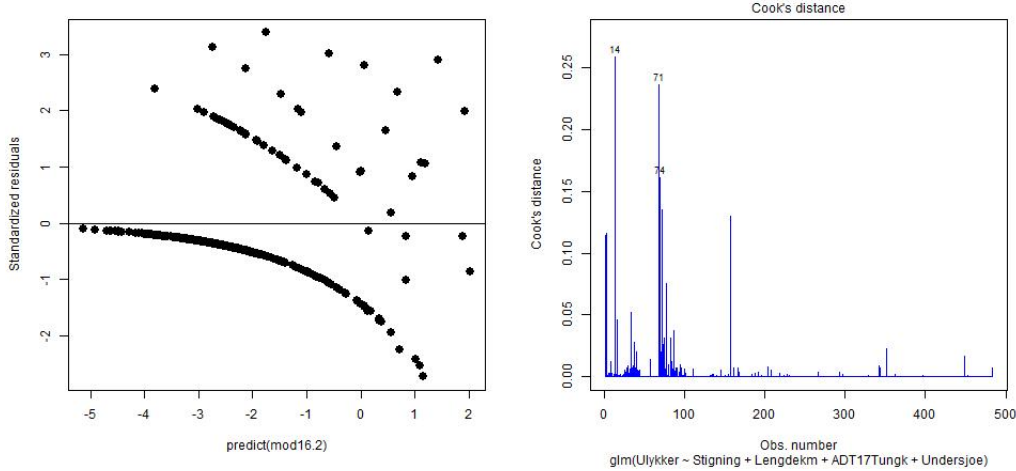
Figure 18: Plot of standardized deletion residuals vs. $\boldsymbol{x}_i\hat{\boldsymbol{\beta}}$ and Cooks distance without the Lærdal tunnel and the Vålerenga tunnel

A new Norwegian subsea tunnel is under construction, called the Ryfast tunnel. The tunnel will have a slope and length of 7% and 13.95 km, respectively. According to KS2 (2011) (Quality Assurance study), the AADT has been estimated to be 4200, where approximately 10% will be heavy goods vehicles. Let us test the model for this particular tunnel, and see if we can predict the number of accidents in the Ryfast tunnel the next 15 years. By using equation 7.2 with estimated parameters found in table 7, we get

$$\mu = \exp(-3.61 + 0.14 \cdot 7 + 0.34 \cdot 13.95 + 0.63 \cdot 0.42 + 1.22) = 36.51$$

More than 2 accidents each year the next 15 years seems highly unlikely. Why does this happen?

According to the model, the effect of length is exponential. The Ryfast tunnel is an extreme tunnel compared to other tunnels in the model. It is subsea and longer than any other tunnel in our data. With these attributes, the Ryfast tunnel would be considered an outlier in the model. However, we could try to overcome this issue by transforming one or more of the covariates by a function of the covariates best fit to even out these covariates, $x_i \rightarrow f(x_i)$. Polynomial and logarithmic functions are strong candidates. By analysing the model found in table 6, the logarithmic function seems to be the best candidate. Transforming length may produce a model that

better fits longer tunnels. I.e, we now test the model

$$\lambda_i = e^{\beta_0 + \beta_1 \log(Length) + \beta_2 AADT + \beta_3 Subsea}$$

We will start by including all tunnels, thus the Lærdal tunnel and the Vålerenga tunnel is included.

The ratio between the length of the longest and the second longest tunnel was 2.14. After this transformation, the ratio has been reduced to 1.31. Thus, the effect of length has been considerably reduced and given us a better representation of the data. The transformation yields the following results

Variable	$\hat{\beta}$	p-value	Rate ratio	95% confidence interval
(Intercept)	-3.36	< 0.0001	-	-
Slope	1.12	0.0081	1.12	1,03, 1.22
log(Length[km])	1.20	< 0.0001	3.32	2.64, 4.18
AADT HGV[1000]	0.57	< 0.0001	1.77	1.62, 1.95
Subsea	1.07	0.0011	2.92	1.53, 5.57

Table 8: Transformed length in the model found in table 6
Number of observations: 485, offset: Number of years with data.
$AIC = 463.81$

We will now compare models and try to minimize the AIC value. By examining the model found in table 6 using different functions mentioned earlier, the logarithmic function, once again, gives the smallest AIC. The smallest AIC is obtained by transforming both length and AADT HGV by log(Length) and log(AADT HGV), respectively. The AIC is reduced from 494.99 to 413.02, meaning the log-likelihood has been reduced from $l(\boldsymbol{\beta}) = -242.50$ to $l(\boldsymbol{\beta}) = -201.51$. The transformation yields the following results

Variable	$\hat{\beta}$	p-value	Rate ratio	95% confidence interval
(Intercept)	-2.32	< 0.0001	-	-
Slope	0.19	< 0.0001	1.21	1.12, 1.31
log(Length[km])	1.15	< 0.0001	3.16	2.50, 3.99
log(AADT HGV[1000])	0.97	< 0.0001	2.64	2.24, 3.08
Subsea	0.57	0.0457	1.77	1.01, 3.08

Table 9: Transformed length and annual average daily traffic in table 6
Number of observations: 485, offset: Number of years with data.
$AIC = 413.02$

It is worth mentioning that the rate ratio for log-transformed covariates does not exactly mean the same thing as the usual covariates. By deriving equation 7.4 with $x_{ik} \to \log x_{ik}$ and $a \to \log a$, we find that predicted number of fire incidents increase by e^{β_k} as x_{ik} increases by $e^1 \cdot a$, and not $a + 1$.
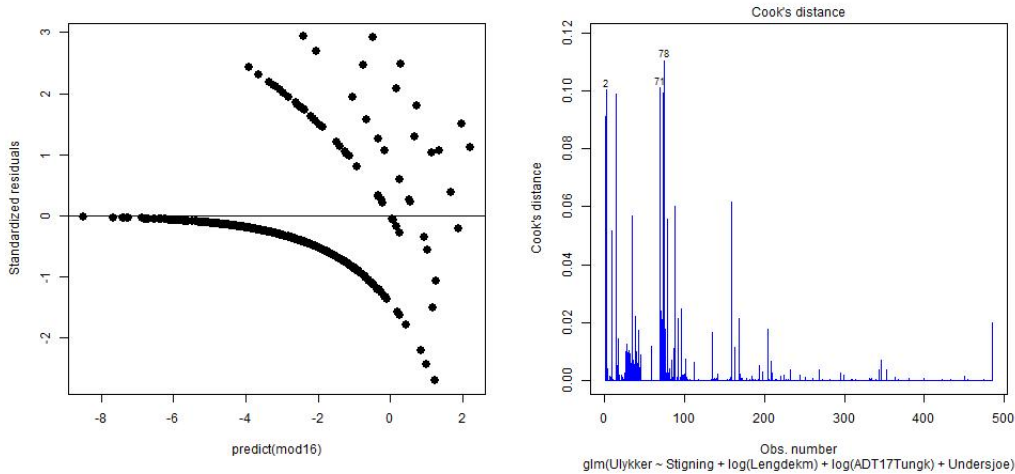
Figure 19: Plot of standardized residuals vs. predicted $\boldsymbol{x}_i\hat{\boldsymbol{\beta}}$ and Cooks distance for the model in table 9

Recall that the Lærdal and the Vålerenga tunnels are included in the log-transform model, and thus also included in the residual plot. The Lærdal tunnel that had Cooks distance $D_i > 40$, is now reduced to less than 0.10. The Lærdal and the Vålerenga tunnels are no longer an issue, and we shall continue modelling with both included.

Predicting incidents in the Ryfast tunnel using the new results found in table 9

$$\mu = \exp(-2.32 + 0.19 \cdot 7.00 + 1.15 \log 13.95 + 0.97 \log 0.42 + 0.57) = 5.87$$

which seems more reasonable.

8.3 Poisson regression model 2

In the second model, we are going to estimate accidents per unit length using the covariates described in section 8.1, with Number of years with data and length as exposure parameters.

$$E(Y_i) = t_{1i}t_{2i}\lambda_i = L_i N_i \lambda_i$$

where L_i is the length of each tunnel and N_i is the number of years with data for each tunnel.

Then for a given tunnel, λ_i models the expected number of accidents per 15 years per km tunnel. I.e $L_i = 1$ for 1 km and $N_i = 1$ for 15 years. The modelling will be done in a similar fashion as the first model. We will start of by estimating each covariate separately. Note that length is now an exposure parameter, rather than a covariate, and will therefore be treated as such.

Variable	$\hat{\beta}$	p-value	Rate ratio	95% confidence interval
Slope	0.21	< 0.0001	1.24	1.16, 1.33
Subsea	1.51	< 0.0001	4.50	2.75, 7.37
AADT[1000]	0.07	< 0.0001	1.07	1.05, 1.08
AADT HGV[1000]	0.49	< 0.0001	1.63	1.48, 1.80
Slope downward	0.21	< 0.0001	1.23	1.15, 1.31
Slope upward	0.24	< 0.0001	1.27	1.17, 1.38

Table 10: Each variable estimated separately.
Number of observations: 485; offset: Number of years with data and Length.

Notice, once again, all parameters when estimated separately, are very significant. The effect of subsea is still substantially larger than other covariates, though a lot less extreme than in the first model.

One way to think about this is that both models estimate parameters such

that for each tunnel the predicted number of accidents gets as close to the observed accidents, $\mu_{i_1} \simeq Y_i$ and $\mu_{i_2} \simeq Y_i$, although they are not necessarily equal to each other. Since the second model has two exposure parameters, it will have an expected number of accidents $\mu_{i_2} = L_i N_i \lambda_{i_2}$, whereas the first model will have $\mu_{i_1} = N_i \lambda_{i_1}$. We have $\lambda_{i_1} = \frac{\mu_{i_1}}{N_i}$ and $\lambda_{i_2} = \frac{\mu_{i_2}}{L_i N_i}$. Then

- for all $L_i > 1$, $\lambda_{i_1} > \lambda_{i_2} \Leftrightarrow \beta_{0_1} + \beta_{1_1} x_1 > \beta_{0_2} + \beta_{1_2} x_1$

- for all $L_i < 1$, $\lambda_{i_1} < \lambda_{i_2} \Leftrightarrow \beta_{0_1} + \beta_{1_1} x_1 < \beta_{0_2} + \beta_{1_2} x_1$

where $x_1 = 1$ for subsea tunnels and $x_1 = 0$ for non-subsea tunnels.

30 subsea tunnels have $L_i > 1$, thus $\beta_{0_1} + \beta_{1_1} > \beta_{0_2} + \beta_{1_2}$.
1 subsea tunnel have $L_i < 1$, thus $\beta_{0_1} + \beta_{1_1} < \beta_{0_2} + \beta_{1_2}$.
Non-subsea tunnels have either $\beta_{0_1} > \beta_{0_2}$ (if $L_i > 1$), $\beta_{0_1} < \beta_{0_2}$ (if $L_i < 1$). Since most subsea tunnels contributes to $\beta_{0_1} + \beta_{1_1} > \beta_{0_2} + \beta_{1_2}$, it is very unlikely that $\beta_{1_2} > \beta_{1_1}$. The only way this could happen is if $\beta_{0_1} \gg \beta_{0_2}$, which is not likely because 40% of the tunnels have $L_i < 1$.

Estimating all parameters simultaneously and eliminating insignificant variables similarly to what we did in Section 8.2 yields the following results presented in table 11.

Variable	$\hat{\beta}$	p-value	Rate ratio	95% confidence interval
(Intercept)	-3.16	< 0.0001	-	-
Slope	0.12	0.0077	1.12	1.03, 1.22
Subsea	1.20	< 0.0001	3.32	1.77, 6.21
AADT HGV[1000]	0.57	< 0.0001	1.76	1.61, 1.93

Table 11: Each variable estimated simultaneously and excluded insignificant variables.
Number of observations: 485; offset: Number of years with data and Length.
$AIC = 464.70$

Compared to the first model (table 6), the results in table 11 does not contain any outliers, see figure 20.
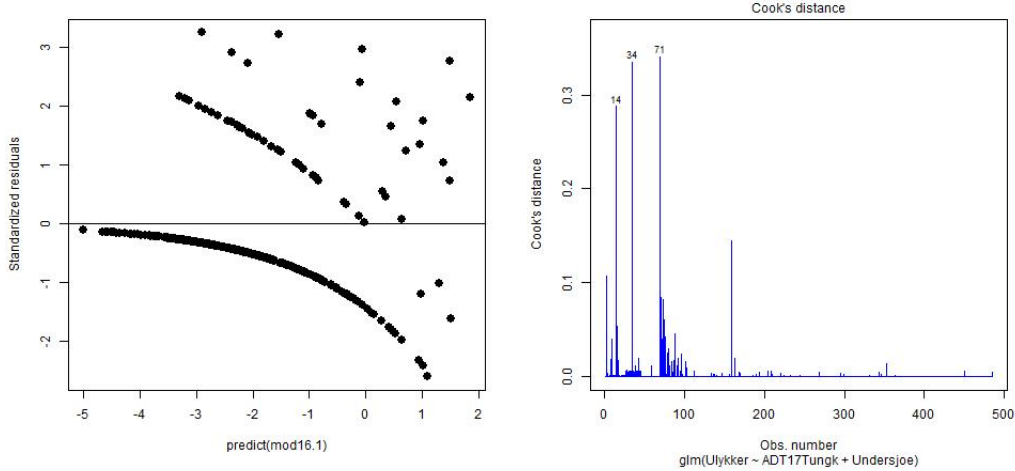
Figure 20: Plot of standardized deletion residuals vs. $\boldsymbol{x}_i\hat{\boldsymbol{\beta}}$ and Cooks plot.

The AIC of the model is 464.70. However, we may try to reduce this by the same method as in Section 8.2. Transforming AADT by log-AADT, and running the elimination process we get the following results.

Variable	$\hat{\beta}$	p-value	Rate ratio	95% confidence interval
(Intercept)	-2.19	< 0.0001	-	-
Slope	0.19	< 0.0001	1.21	1.12, 1.31
Subsea	0.69	0.0108	1.99	1.17, 3.38
log(AADT HGV)	0.96	< 0.0001	2.62	2.22, 3.08

Table 12: Transformed AADT HGV in table 11
Number of observations: 485; offset: Number of years with data and Length.
$AIC = 412.58$

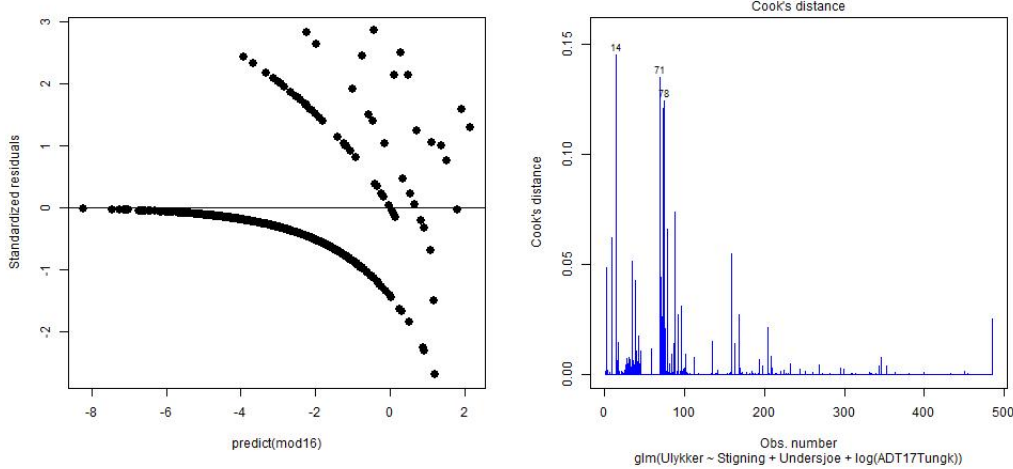The corresponding residuals and Cooks plots are found in figure 21

Figure 21: Plot of standardized deletion residuals vs. $\boldsymbol{x}_i\hat{\boldsymbol{\beta}}$ and Cooks plot.

Note how similar the AIC of this model is compared to the AIC of the first model found in table 9. This raise the question; Which model is the better model. How do they compare?

8.4   Comparison of models

We will first compare the first model with the exponential effect of length found in table 6 and the second model found in table 11. We will thereafter compare the first model with log-transform in table 9 and the second model with log-transform in table 12.

Although both models end up with the same variables in the final result, the main difference between the the two models is that the first model has an exponential function of length (not including the log-transform model), while the second model does not. For illustration purposes; while we compare the two models, let α_i denote parameters in the first model, and β_i denote parameters in the second model.

$$\mu_{i_{mod1}} = N_i e^{\alpha_0 + \alpha_1 s_i + \alpha_2 L_i + \alpha_3 A_i + \alpha_4 S_i} \tag{8.1}$$

and

$$\mu_{i_{mod2}} = L_i N_i e^{\beta_0 + \beta_1 s_i + \beta_2 A_i + \beta_3 S_i} \tag{8.2}$$

where s_i, L_i, N_i, A_i and S_i are the $i'th$ slope, length, number of years with data, AADT HGV and subsea variables, respectively.

63

Suppose we want to compare the rate of accidents as a function of length for the two models. First, notice that the parameter for intercept, slope and AADT HGV[1000] are equal in both models (at least for 2 decimal places), see table 6 and 11. Thus,

$$\alpha_0 + \alpha_1 s_i + \alpha_3 A_i = \beta_0 + \beta_1 s_i + \beta_2 A_i$$

Using this when comparing the rate of accidents for both models found in equation 8.1 and 8.2, we can find the lengths that produce equal predicted number of accidents in subsea and non-subsea tunnels for both models.
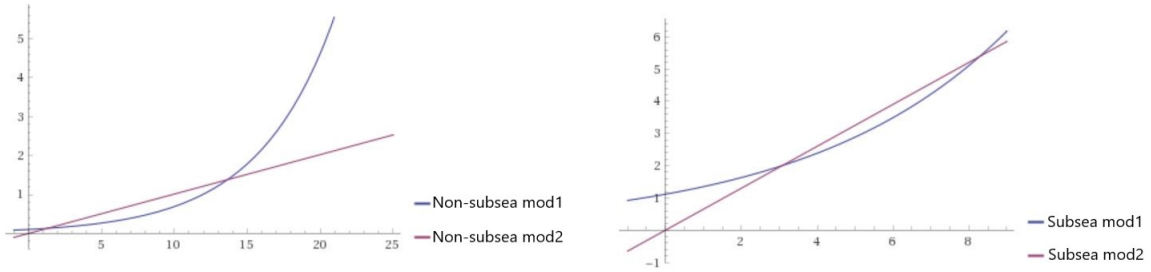

Figure 22: Estimated accidents as a function of length for both models

The lengths where the estimated fire accidents in the first model intersects the estimated fire accidents in the second model.

$$\mu_{mod1} = \mu_{mod2} \tag{8.3}$$
$$e^{\alpha_2 L + \alpha_4 S_i} = L e^{\beta_3 S_i}$$

which gives us the following equation.

$$\alpha_2 L - \ln(L) + (\alpha_4 - \beta_3)S_i = 0 \tag{8.4}$$

Since a tunnel is either subsea or not, we will only need to consider two cases, $S_i = 0$ and $S_i = 1$

Case 1: Non-subsea tunnels$(S_i = 0)$
Using equation 8.4 with $S_i = 0$, we get

$$\alpha_2 L - \ln(L) = 0 \tag{8.5}$$

Equation 8.5 has two solutions and can either be solved by graphing or by using the Lambert W-function, which is the inverse function of $f(x) = xe^x$. Solve equation 8.5, we get

$$L = e^{\alpha_2 L}$$

$$-\alpha_2 L e^{-\alpha_2 L} = -\alpha_2$$

which is of the form xe^x. Apply the Lambert W-function

$$-\alpha_2 L = W(-\alpha_2)$$

such that

$$L = e^{-W(-\alpha_2)} \tag{8.6}$$

The Lambert W-function has the series expansion (Eric W. Weisstein, 2019)

$$W(x) = \sum_{n=1}^{\infty} \frac{(-1)^{n-1} n^{n-2}}{(n-1)!} x^n \tag{8.7}$$

and has real values for $x > -\frac{1}{e}$.

Using the first 7 terms with $x = -\alpha_2 = -0.19$ gives a good approximation of $W(-\alpha_2)$. Substituting the result into equation 8.6 produce the first solution to equation 8.5

$$L_1 = 1.27$$

The second solution is found by analytic continuation of the lambert W-function, $W_{-1}(-\alpha_2)$. Without too much details, the solution is given below

$$L_2 = 13.82$$

What this means is that non-subsea tunnels with lengths $L = 1.27$ or $L = 13.82$ have the same predicted accidents in the first and second model. Also, equation 8.5 is negative for $L_i \in (1.27, 13.82)$, which means that the rate of accidents in tunnels with lengths between 1.27 km and 13.82 km is greater in the second model than the first model. Moreover, equation 8.5 is positive for $L_i < 1.27$ and $L_i > 13.82$, which means that the first model has more predicted accidents in these domains.

Equation 8.5 has a global minima for $L = 5.26$km, which means the biggest difference in the two models on the interval $L_i \in (1.27, 13.82)$ is $L = 5.26$. Also, since

$$\lim_{L \to \infty} \alpha_2 L - \ln(L) = \infty$$

the predicted accidents of tunnels longer than 13.82 km gets increasingly larger for the first model compared to the second model as the length increases. The same argument goes for $L < 1.27$ km, since

$$\lim_{L \to 0} \alpha_2 L - \ln(L) = \infty$$

the difference in predicted accidents increases as length decrease. However, the model is restricted to tunnels longer than 500 m, so this limit is not realistic. If $L = 0$, the second model will have $\mu_{mod2} = 0$, whereas the first model will have $\mu_{mod1} \neq 0$, thus μ_{mod1} can not equal μ_{mod2}.
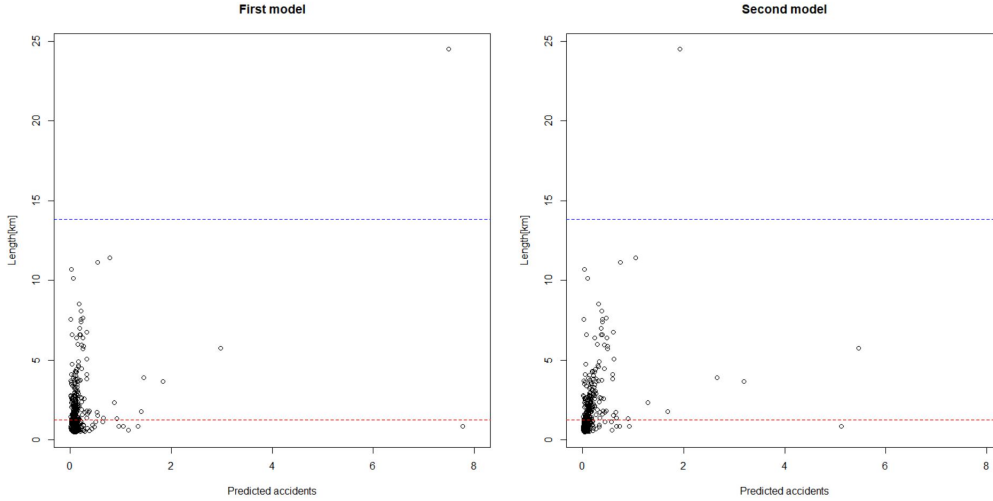

Figure 23: Predicted accidents in non-subsea tunnels per length km for the first and second model. Red line represents $L_1 = 1.27$ and blue line represents $L_2 = 13.82$.

Figure 23 clearly shows that tunnels above the blue line and below the red line have more predicted accidents in the first model compared to the second model, especially Lærdal tunnel as it is furthest away from the blue line. Furthermore, points between the red and blue line have more predicted accidents in the second model, as expected. The greatest difference is for points around 5 km on the y-axis.

Case 2: Subsea tunnels$(S_i = 1)$
Using equation 8.4 with $S_i = 1$, we get

$$\alpha_2 L - \ln(L) + (\alpha_4 - \beta_3) = 0 \qquad (8.8)$$

Equation 8.8 can either be solved numerically or by graphing. The solutions are

$$L_1 = 3.08$$

and

$$L_2 = 8.29$$

66

The function $f(L) = \alpha_2 L - \ln(L) + (\alpha_4 - \beta_3)$ has a global minima for $L = 5.26$. However, since $f(5.26) = -0.12$ both models are approximately equal for all $L_i \in (3.08, 8.29)$. The small deviation can be seen in figure 24. Notice, the only point that is "substantially" different in the second model is the point furthest below the red line.

Figure 24: Predicted accidents in subsea tunnels per length km for the first and second model. Red line represents $L_1 = 3.08$ and blue line represents $L_2 = 8.29$.

Comparing log-transform models
We will now compare the log-transform models found in table 9 and 12, by the same method. Both models end up with the same variables in the final result, only this time the first model does not have an exponential function of length.

We let α_i denote parameters in the first model, and β_i denote parameters in the second model.

$$\mu_{i_{mod1}} = L_i^{\alpha_2} A_i^{\alpha_3} N_i e^{\alpha_0 + \alpha_1 s_i + \alpha_4 S_i} \tag{8.9}$$

and

$$\mu_{i_{mod2}} = L_i A_i^{\beta_2} N_i e^{\beta_0 + \beta_1 s_i + \beta_3 S_i} \tag{8.10}$$

Note that the parameter for slope are equal, and the parameter for AADT

HGV are almost equal in both models, see table 9 and 12. Thus,

$$\alpha_1 s_i + \alpha_3 \log(A_i) \simeq \beta_1 s_i + \beta_2 \log(A_i)$$

Using this when comparing the rate of accidents for both models found in equation 8.9 and 8.10, we can find the lengths that produce equal predicted number of accidents in subsea and non-subsea tunnels for both log-transform models.

Figure 25: Estimated accidents as a function of length for both log-transformed models.

Notice that these functions are even more similar, especially for subsea tunnels. Moreover, we do not get that exponential growth seen for non-subsea tunnels in figure 22. By setting equations 8.9 and 8.10 equal to each other, we get

$$L_i^{\alpha_2} e^{\alpha_0 + \alpha_4 S_i} = L_i e^{\beta_0 + \beta_3 S_i} \tag{8.11}$$

which has a unique solution (not including $L = 0$) for non-subsea tunnels

$$L = 2.38$$

and for subsea tunnels

$$L = 5.29$$

Since equation 8.11 is almost flat for all $L_i \in (0.5, 24.5)$ for non-subsea tunnels and for all $L_i \in (0.5, 8.9)$ for subsea tunnels, both models are almost identical for all tunnels in our dataset. The largest difference is the Lærdal tunnel, which only differs by 1.04 in these two models. Alternatively, we could have argued that since 1 is included in the confidence interval of $\alpha_2 \in (0.92, 1.38)$, the second model is included in the first model.

The corresponding length versus predicted accidents for non-subsea and subsea tunnels can be found in figure 26 and 27, respectively.

Figure 26: Predicted accidents in non-subsea tunnels per length km for the first and second log-transformed models. Blue line represents $L = 2.38$.
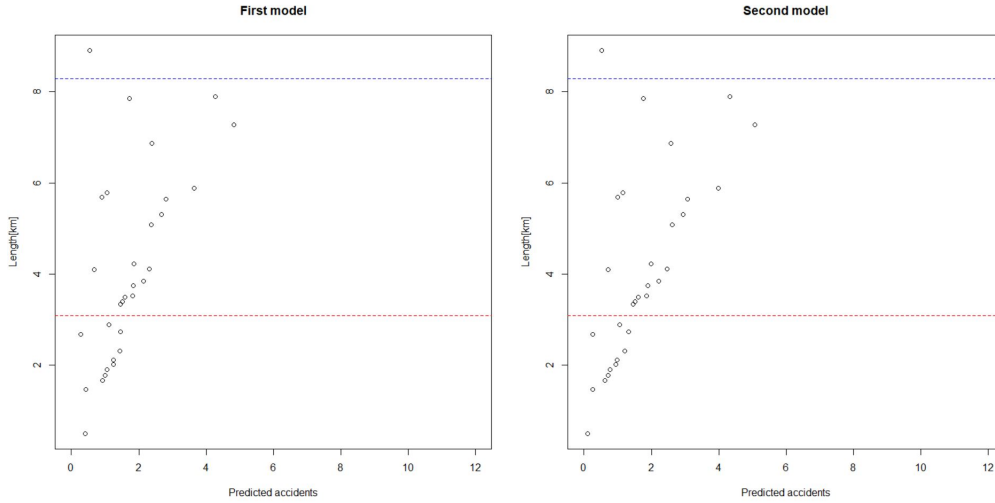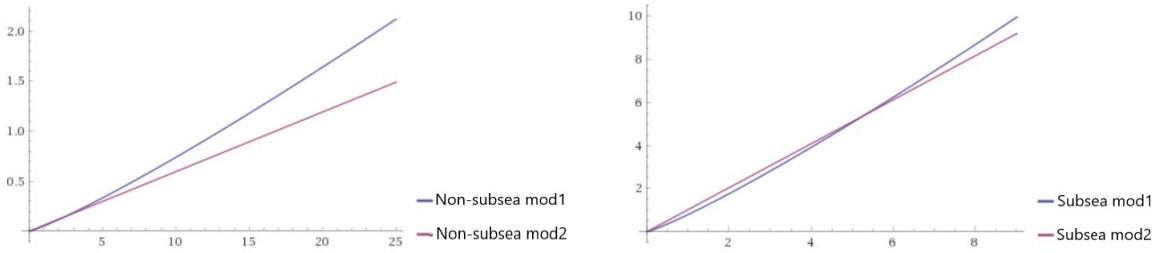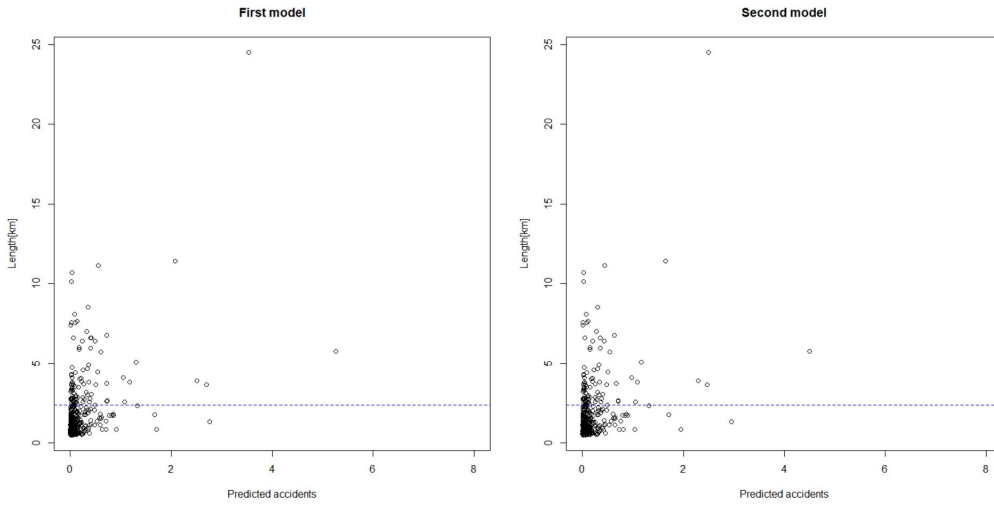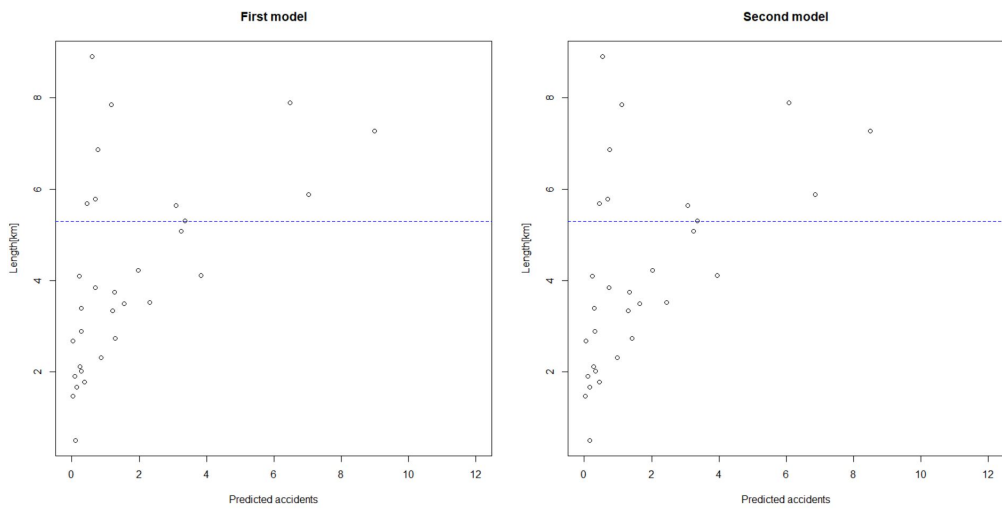

Figure 27: Predicted accidents in subsea tunnels per length km for the first and second models. Blue line represents $L = 5.29$.

9 Sub-models

It may be interesting to classify tunnels based on some properties we wish to examine, and see if the circumstances are the same in interesting subgroups compared to the entire dataset. So, in this section, we are going to consider various subsets of our dataset, perform regression analysis and compare them to what we analysed in Sections 8.2 and 8.3, as well as each other. Since the log-transform models found in table 9 and 12 gave the best fit, we will primarily consider these models when we compare the models. Note that we only present the final results for each case. That is, the results obtained after evaluation and elimination. The resulting tables can be found in the appendix.

9.1 Subsea versus non-subsea tunnels

Subsea and non-subsea tunnels have been investigated by the same modelling as previously conducted. As only 31 out of 485 tunnels are subsea, the dataset of subsea tunnels has been severely reduced, and may consequently affect the significance of the factors included in subsea model. Non-subsea tunnels, however, should not be affected by observational inadequacy.
The results for subsea tunnels can be found in table 21 and 22 in the appendix. We see that the effect of AADT HGV has been increased for both models compared to the effect of AADT HGV in the complete dataset, see table 6 and 11. This needs further investigation, see Section 10.

Note that slope is no longer a significant covariate. Because subsea tunnels are particularly steep, there is only a small variation of slope in subsea tunnels. Due to this small variation, and also due to few observations, slope is an insignificant covariate in the model containing only subsea tunnels.

The results for non-subsea tunnels in table 23 and 24 can be found in the appendix. Compared to the results of the whole dataset, we see only marginal differences. The effect of AADT and Length has been slightly reduced, as a result of fewer extreme observations.

9.2 Tunnels longer than 4 km versus tunnels shorter than 4 km

Tunnels longer and shorter than 4 km has been investigated by the same modelling as previously conducted. Similarly to subsea tunnels, only 51 out of 485 tunnels are longer than 4 km, which again may affect the significance of parameters in the model containing tunnels longer than 4 km. The results for tunnels longer than 4 km can be found in table 25 and 26 in the appendix. We do not see any drastic changes compared to the results found in table 6 and 11. Surprisingly, length is still significant. One would assume that there would not be as much variation of length for tunnels longer than 4 km, essentially making length insignificant. Though, this is not the case.

The results for tunnels shorter than 4 km in table 27 and 28 can be found in the appendix. Note that subsea is no longer significant. 17 subsea tunnels are shorter than 4 km, and only 2 tunnels have had fire accidents (2 accidents in Fannefjord tunnel and 1 accident in Skatestraum tunnel). This may indicate that the risk of fire accidents in short subsea tunnels is low. Though, this needs further investigation, see Section 10.

10 Comparison of results

In this section we shall try to get a better understanding of the results from sub-models in Section 9 by comparing them to what we analysed in Sections 8.2 and 8.3.

We will start off by comparing parameters of model 1 and various sub models. All parameters are estimated in univariate models.

Variable	Model 1	Subsea	Non-subsea	L > 4 km	L < 4 km
Slope	0.27 ***	-0.48 .	0.18 **	0.34 ***	0.10 .
Length[km]	0.17 ***	0.51 ***	0.14 ***	0.04	0.51 ***
log(Length)	1.26 ***	2.65 ***	0.90 ***	0.54 .	1.02 ***
Subsea	2.34 ***	-	-	2.08 **	0.17
AADT[1000]	0.05 ***	0.28 ***	0.07 ***	0.10 ***	0.07 ***
AADT HGV[1000]	0.43 ***	2.38 ***	0.52 ***	0.55 ***	0.49 ***
log(AADT HGV)	0.68 ***	1.39 ***	0.78 ***	1.21 ***	0.70 ***
Slope downward	0.31 ***	0.03	0.25 *	0.31 ***	0.06
Length downward[km]	0.33 ***	1.14 ***	0.21 *	0.14	0.48
Slope upward	0.26 ***	-0.12	0.14 *	0.38 ***	0.09
Length upward[km]	0.27 ***	0.81 ***	0.25 ***	-0.11	0.50 **

Table 13: Parameter estimates of univariate Model 1 and various univariate sub-models
Significance levels: 0.0001 '***' 0.001 '**' 0.01 '*' 0.05 '.' 0.1 ' '

Notice the effect of AADT HGV is substantially larger for subsea tunnels compared to non-subsea tunnels. Increasing annual average daily traffic of HGV by 1000 in a subsea tunnel will result with an increase of 10.8 accidents, compared to 1.68 accidents in a non-subsea tunnel. This raise the question to whether it is necessary to authorize a control system of how many HGVs are permitted through a subsea tunnel each day.

Also, notice the negative effect of slope in the subsea model. Although insignificant (p-value = 0.0709), this result may indicate that slope decrease the number of fire accidents in subsea tunnels. Subsea tunnels are particularly steep, as it is one of their main attributes. Due to small variation in slope combined with steeper subsea tunnels seems to have less fire accidents, explains the negative slope parameter. However, we can not conclude that fire accidents are less likely to occur in steeper subsea tunnels, and therefore

recommend building tunnels as steeply as possible, as this would contradict not only what we have talked about in this thesis, but also with rational belief. There is no reason to believe that this is a real effect.

Furthermore, the effect of subsea for short tunnels have decreased drastically as we discussed in Section 9.2.

Compare parameters of model 2 and various sub-models.

Variable	Model 2	Subsea	Non-subsea	L > 4 km	L < 4 km
Slope	0.21 ***	-0.51 *	0.22 ***	0.37 ***	0.08
Subsea	1.51 ***	-	-	2.23 **	-0.54
AADT[1000]	0.07 ***	0.28 ***	0.08 ***	0.11 ***	0.07 ***
AADT HGV[1000]	0.49 ***	1.92 ***	0.56 ***	0.57 ***	0.51 ***
log(AADT HGV)	0.80 ***	1.15 ***	0.89 ***	1.25 ***	0.73 ***
Slope downward	0.21 ***	0.04	0.23 *	0.32 ***	-0.02
Slope upward	0.24 ***	-0.02	0.19 **	0.43 ***	0.09 .

Table 14: Parameter estimates of univariate Model 2 and various univariate sub-models
Significance levels: 0.0001 '***' 0.001 '**' 0.01 '*' 0.05 '.' 0.1 ' '

Again, the effect of AADT is substantially larger for subsea tunnels and the slope parameter for subsea tunnels is negative.

Since some of the variables seems to have different effects for different subsets of the data, we may want to consider performing an analysis of the models where we include an interaction term between certain variables.

10.1   Interaction

The first model, which is the model predicting fire accidents per tunnel is examined using the interaction of AADT and subsea. The results are given in table 15

Variable	$\hat{\beta}$	p-value	Rate ratio	95% confidence interval
(Intercept)	-1.14	< 0.0001	-	-
log(AADT HGV)	0.78	< 0.0001	2.18	1.82, 2.62
Subsea	2.98	< 0.0001	19.67	13.47, 28.71
log(AADT HGV) · Subsea	0.61	0.0069	1.84	1.18, 2.85

Table 15: Interaction of AADT and subsea.
Number of observations: 485, offset: Number of years with data.
$AIC = 505.84$

Since $\mu_i = t_i e^{\hat{\beta}_0 + \hat{\beta}_1 \log A_i + \hat{\beta}_2 S_i + \hat{\beta}_3 \log A_i \cdot S_i}$, where A_i is AADT HGV for tunnel i and $S_i = 0$ for non-subsea tunnels and $S_i = 1$ for subsea tunnels, we interpret these results the following way

- The effect of log(AADT HGV) in subsea tunnels is the combined effect of log(AADT HGV) and log(AADT HGV) · Subsea ($\hat{\beta}_1 + \hat{\beta}_3 = 0.78 + 0.61 = 1.39$)

- The effect of log(AADT HGV) in non-subsea tunnels is the effect of log(AADT HGV) ($\hat{\beta}_1 = 0.78$)

These are the same results as the results for log(AADT HGV) in subsea and non-subsea tunnels given in table 13.

Also, since the interacting terms are very significant, it give us more evidence to believe that subsea tunnels are more exposed to AADT HGV.

We have seen that the effect of subsea tunnels is minuscule for subsea tunnels shorter than 4 km compared to long subsea tunnels. We shall therefore examine the model by interaction of length and subsea. The results are given in table 16

Variable	$\hat{\beta}$	p-value	Rate ratio	95% confidence interval
(Intercept)	-2.08	< 0.0001	-	-
log(Length)	0.90	< 0.0001	2.46	1.92, 3.16
Subsea	-1.29	0.0857	0.28	0.06, 1.20
log(Length) · Subsea	1.74	< 0.0001	5.72	2.46, 13.31

Table 16: Interaction of length and subsea.
Number of observations: 485, offset: Number of years with data.
$AIC = 558.38$

Although insignificant, the subsea parameter alone does not considerably contribute to the estimated fire accidents. Hypothetically, a subsea tunnel with zero length has a decreasing effect on the rate of fire accidents $(\hat{\beta}_0 + \hat{\beta}_2 = -3.37)$. However, because of the significant interaction of length and subsea, there is a significant effect of subsea. The parameter estimate of subsea increase with length $\hat{\beta} = \hat{\beta}_2 + (\hat{\beta}_1 + \hat{\beta}_3) \log L_i = -1.29 + 2.64 \log L_i$. It seems that the effect of subsea tunnels will only start to significantly increase the risk of fire accidents as the subsea tunnel gets sufficiently long $(L_i > 3.58 \text{ km})$.

It may also be interesting to include these two interaction models in the models that gave the best fit in Section 8.2 and 8.3. We will start by including interactions in table 9, and table 12 thereafter.

Including interaction in the first model
By including interaction of AADT and Length with subsea, we get the following results

Variable	$\hat{\beta}$	p-value	Rate ratio	95% confidence interval
(Intercept)	-2.29	< 0.0001	-	-
Slope	0.21	< 0.0001	1.24	1.14, 1.34
log(Length)	1.04	< 0.0001	2.85	2.22, 3.67
log(AADT HGV)	0.87	< 0.0001	2.39	1.99, 2.88
Subsea	-0.53	0.569	0.59	0.09, 3.66
log(Length) · Subsea	0.69	0.169	2.00	0.74, 5.39
log(AADT HGV) · Subsea	0.35	0.165	1.42	0.87, 2.32

Table 17: Interaction of length and AADT with subsea included in table 9. Number of observations: 485, offset: Number of years with data. $AIC = 410.68$

We see that subsea becomes insignificant as a result of what we observed in table 16. Also, neither length nor AADT HGV have a significant interaction with subsea, thus we eliminate the least significant interaction. By eliminating the interaction of length and subsea, we get

Variable	$\hat{\beta}$	p-value	Rate ratio	95% confidence interval
(Intercept)	-2.34	< 0.0001	-	-
Slope	0.21	< 0.0001	1.24	1.14, 1.34
log(Length)	1.10	< 0.0001	3.00	2.36, 3.81
log(AADT HGV)	0.88	< 0.0001	2.41	2.00, 2.90
Subsea	0.67	0.0159	1.96	1.13, 3.38
log(AADT HGV) · Subsea	0.48	0.0437	1.62	1.01, 2.59

Table 18: Eliminated the interaction of length and subsea from table 17.
Number of observations: 485, offset: Number of years with data.
$AIC = 410.68$

Notice that without the interaction of length and subsea, subsea is once again significant. This further supports our assumption, that short subsea tunnels are not considered as influential compared to long subsea tunnels.

The corresponding residuals and Cooks plots can be found in figure 28.
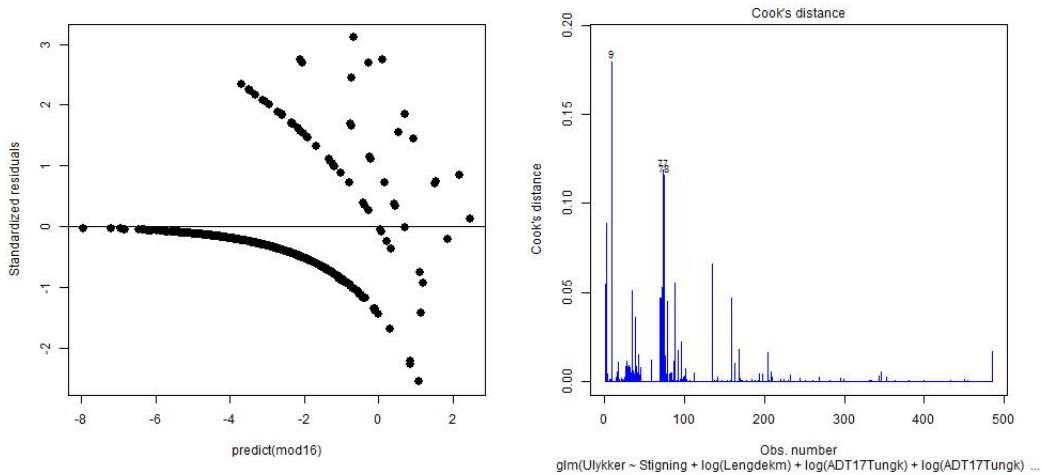

Figure 28: Plot of standardized deletion residuals vs. $\boldsymbol{x}_i\hat{\boldsymbol{\beta}}$ and Cooks plot.

Since both interaction variables in table 17 have almost identical p-values, we could just as well excluded the interaction of AADT HGV and subsea. By doing so, we get the following result

Variable	$\hat{\beta}$	p-value	Rate ratio	95% confidence interval
(Intercept)	-2.26	< 0.0001	-	-
Slope	0.20	< 0.0001	1.22	1.13, 1.32
log(Length)	1.06	< 0.0001	2.89	2.25, 3.72
log(AADT HGV)	0.93	< 0.0001	2.53	2.14, 3.00
Subsea	-1.02	0.2400	0.36	0.07, 1.97
log(Length) · Subsea	0.93	0.0473	2.54	1.01, 6.40

Table 19: Eliminated the interaction of AADT HGV and subsea from table 17.
Number of observations: 485, offset: Number of years with data.
$AIC = 410.72$

Notice that the rate of fire accidents increases approximately linearly with length for non-subsea tunnels ($\hat{\beta}_2 = 1.06$), while it increases approximately quadratically for subsea tunnels ($\hat{\beta}_2 + \hat{\beta}_5 = 1.99$). Thus, doubling the length of a non-subsea tunnel should double the rate of accidents, while doubling the length of a subsea tunnel should quadruple the rate of accidents. The corresponding residuals and Cooks plots can be found in figure 29.
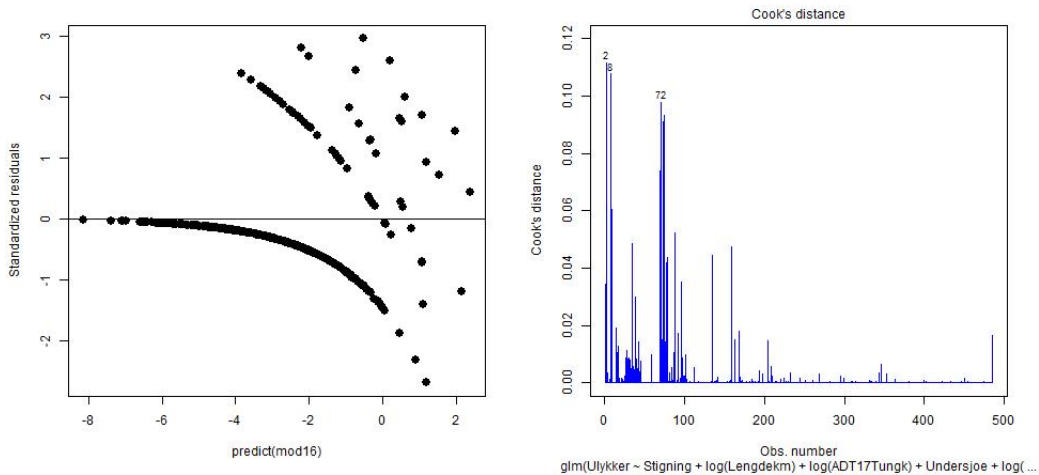
Figure 29: Plot of standardized deletion residuals vs. $\boldsymbol{x}_i\hat{\boldsymbol{\beta}}$ and Cooks plot.

Including interaction in the second model
AADT HGV seems to have a greater effect on subsea tunnels in the second model also, see table 14. We will therefore analyse the interaction of AADT

HGV and subsea for the second model, similarly to what we did for the first model. Since length is an offset in the second model, we will not be able to analyse the interaction of length. Including the interaction of AADT HGV and subsea in table 12, we get

Variable	$\hat{\beta}$	p-value	Rate ratio	95% confidence interval
(Intercept)	-2.26	< 0.0001	-	-
Slope	0.21	< 0.0001	1.24	1.14, 1.34
log(AADT HGV)	0.87	< 0.0001	2.38	1.99, 2.85
Subsea	0.76	0.00283	2.14	1.30, 3.53
log(AADT HGV) · Subsea	0.52	0.02706	1.68	1.06, 2.66

Table 20: Interaction of AADT HGV with subsea included in table 12. Number of observations: 485, offset: Number of years with data and Length. $AIC = 409.30$

Notice in particular the AIC value for each models in table 18, 19 and 20. Since neither model have any influential observations, see Cooks plots for each model, the model which gives the best fit is in table 20.
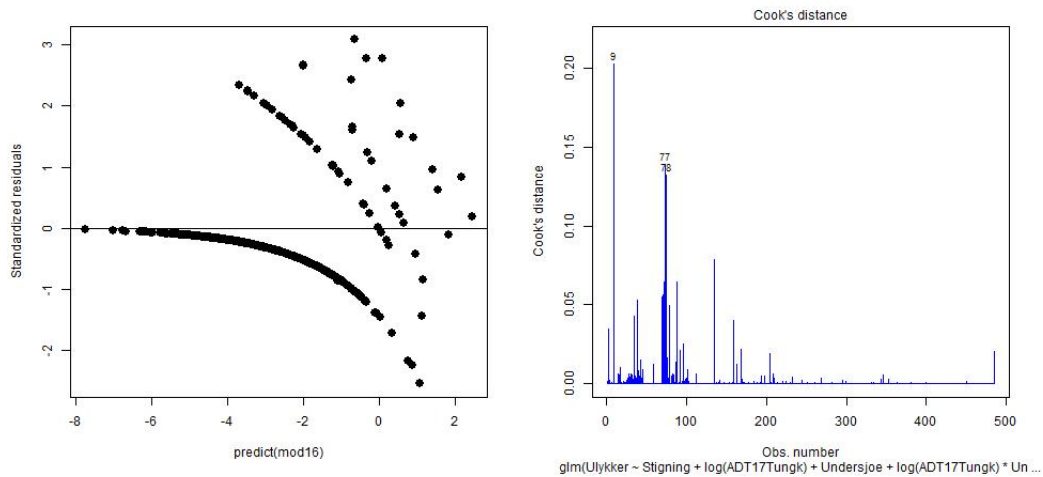

Figure 30: Plot of standardized deletion residuals vs. $\boldsymbol{x}_i\hat{\boldsymbol{\beta}}$ and Cooks plot.

11   Final statistical model

Statistically, the model in table 20 is the best model, and should primarily be used for modelling the rate of fire accidents in Norwegian road tunnels. However, we should also consider the model in table 19 as it captures the interaction of length and subsea. Both models fits the data almost equally.

When estimating fire accidents in tunnels with distinct tunnel characteristics and in particular when one variable differentiate substantially from other tunnels in the data material, the models mentioned above will also vary from one another. In Section 8.2, we estimated fire accidents in the Ryfast tunnel by using the model we had at the time. Estimating fire accidents in the Ryfast tunnel using the model found in table 20, we get

$$\mu = LA^{\hat{\beta}_3 + \hat{\beta}_5} e^{\hat{\beta}_0 + \hat{\beta}_1 s + \hat{\beta}_4 S} = 4.05$$

Estimating fire accidents in the Ryfast tunnel using the model found in table 19, we get

$$\mu = L^{\hat{\beta}_2 + \hat{\beta}_5} A^{\hat{\beta}_3} e^{\hat{\beta}_0 + \hat{\beta}_1 s + \hat{\beta}_4 S} = 12.91$$

Clearly, the predicted fire accidents estimated by the two models is considerably different.

As mentioned in section 10.1, the predicted accidents using the model in table 19 increases approximately quadratically with length. Since the Ryfast tunnel is almost twice as long as the longest tunnel in the data material, we get the same problem as we did with the Lærdal tunnel, only this time due to polynomial growth.

Although both models fits accidents well in the data material, the predictions get problematic when estimating tunnels sufficiently far away from the data material. We are not sure which model we should trust.

For a more practical approach, we should also consider using the model in table 17. Even though the interactions are insignificant, it encapsulate all interactions and might, in some cases, give us a better representation of the predicted fire accidents. Estimating fire accidents in Ryfast tunnel using this model, we get

$$\mu = L^{\hat{\beta}_2 + \hat{\beta}_6} A^{\hat{\beta}_3 + \hat{\beta}_7} e^{\hat{\beta}_0 + \hat{\beta}_1 s + \hat{\beta}_5 S} = 8.59$$

We trust researchers from the risk management field to evaluate and discuss the validity of the models presented here. Together with other studies on risk influencing factors, these researchers can make a qualitative decision of which model we should trust, in particular when estimating fire incidents in tunnels like the Ryfast tunnel. Remember, we have produced estimates on fire incidents risks, not for catastrophic fires as seen for example in the Mont Blanc tunnel in 1999. Such extremely remote events needs careful considerations.

12   Discussion

The statistical modelling shows that the key factors influencing fire accidents in road tunnels are; **slope, length, annual average daily traffic of heavy goods vehicles and whether a tunnel is subsea or not**. These are in accordance to Nævestad and Meyer (2013) speculations, but in this analysis using data from all Norwegian tunnels of length > 0.5km these factors stand out as clearly significant. Moreover, we have been able to evaluate the importance of each factor and how they contribute to fire accidents in road tunnels.

We mentioned in section 3.7, all tunnels investigated by AIBN have at least one distinct tunnel characteristic significant for fire in HGVs. Now that we have established which factors are influential, we see why these tunnels are more exposed to fire occurrences in HGVs.

- The Oslofjord tunnel, which is probably the most extreme of all, is a long, steep subsea tunnel with above average AADT HGV.

- The Gudvanga tunnel is the second longest tunnel in Norway.

- The Skatestraum tunnel is an extremely steep subsea tunnel.

- The Måbø tunnel is an extremely steep tunnel.

In Section 8.1, we used the study Høye et al. (2019) of AADT development for private and freight transport in Norway from 2005 to 2017. We acknowledge that this global representation of AADT development may be a source of error for some individual road tunnels. If a road opens adjacent to a specific road tunnel such that a driver has the opportunity to choose between the two, the global AADT remains the same, however, the AADT for the specific tunnel will decrease, and not linearly as we discussed in Section 8.1. With AADT data for each year, we might have been able to get a better representation of the variable during the modelling activities.

During the introduction, we saw a large variation of accidents in 2001-2007 compared to 2008-2015. We speculated whether the traffic flow has increased so drastically, and thus increased the rate of accidents. According to figure 13, this is not the case. The relative AADT from 2007 to 2015 has only increased by approximately 10%. We believe the reporting system has become better, and is the main reason of the variation of accidents.

However, as stated in the introduction, Elvik and Mysen (1999) have documented weaknesses in the reporting systems, also confirmed by Njå et al. (2008). Police are obligated to report accidents involving injuries to humans. Accidents without major consequences are sometimes ignored by the police, and consequently absent in the reporting system.

Njå (2017) assessed Nævestad's (2016) data material on fires in tunnels with serious outcomes. The data Njå assessed included collisions leading to fires and major consequences to humans. He identified heavy fire loads (heat release rate – HRR) for seven events, of which the fire in the Brattli tunnel lasted for several days and the Skatestraum tunnel fire was estimated to more than 400 MW. A design fire in a bus is defined as 30 MW and a truck on fire is 50-100 MW (Ingason, Li and Lonnermark, 2014). Only a fire in the Follo tunnel includes uncertainties regarding whether a victim died from smoke intoxication or from the collision forces (truck against the tunnel wall at the entrance of the tunnel).

Furthermore, Njå (2017) checked all incidents described in Nævestad's material that included Zero Vision accidents. Three of the ten accidents he scrutinized included erroneous information, which compared to Elvik and Mysen (1999) fits well with their findings. However, Nævestads data of accidents is the best we have, and it should give us a reasonable statistical conclusion of fire in HGVs in road tunnels.

Most fires and near fires included in the data material in this study is reported from various sources, mainly the Police/NPRA and the Fire departments/DSB. Elvik and Mysen (1999) assessed the Police/NPRA data, which is the official data included in the national public statistics (SSB – Statistics Norway). Data from fire departments should be scrutinized because there are reasons to believe that the report practices have changed over the years (from 2001 to 2015). There are several reasons for this:

- The DSB has introduced a new incident reporting system.

- It is important for fire departments to document activities, but the need for accuracy is less important.

- The NPRA is responsible for ensuring sufficient emergency response arrangements, and the fire departments request that the NPRA provide necessary equipment. There has been conflicts of interests amongst

the parties (Njå and Svela, 2018), which might have impacted reporting.

The reliability of the recorded information has not been studied, but there are reasons to believe that there might be weaknesses. For example, the Byfjord tunnel, which has many resemblances with the Oslofjord tunnel, has only near fires recorded. Near fires is an unclear criteria, which is defined as development of smoke but could easily be a situation in which the operator in the road traffic management centre suspect smoke development (Njå, 2017). Elvik and Mysen (1999) experienced huge discrepancies in report practice when the incident outcome was less serious. However, there is no reason to believe that weaknesses in report systems are uneven distributed within Norway, so we could argue that it is not that important. But, since the data material only consist of 131 events, it would have been interesting to pursue this issue in follow up research activities.

We also recommend further research involving; modelling physics and thermodynamics within heavy goods vehicles prior to fire ignition.

Appendices

A   Tables

A.1   Subsea tunnels

Variable	$\hat{\beta}$	p-value	Rate ratio	95% confidence interval
(Intercept)	-1.15	0.1857	-	-
log(Length)	1.73	< 0.0001	5.66	2.25, 14.25
log(AADT HGV)	0.99	< 0.0001	2.70	1.76, 4.12

Table 21: Results from regression model of subsea tunnels.
Number of observations: 31, offset: Number of years with data.
$AIC = 83.43$

Variable	$\hat{\beta}$	p-value	Rate ratio	95% confidence interval
(Intercept)	0.16	0.289	-	-
log(AADT HGV)	1.15	< 0.0001	3.17	2.14, 4.69

Table 22: Results from regression model of subsea tunnels.
Number of observations: 31, offset: Number of years with data and Length.
$AIC = 84.08$

A.2   Non-subsea tunnels

Variable	$\hat{\beta}$	p-value	Rate ratio	95% confidence interval
(Intercept)	-2.29	< 0.0001	-	-
Slope	0.21	< 0.0001	1.23	1.14, 1.34
log(Length)	1.05	< 0.0001	2.85	2.22, 3.67
log(AADT HGV)	0.87	< 0.0001	2.39	1.99, 2.88

Table 23: Results from regression model of non-subsea tunnels.
Number of observations: 454, offset: Number of years with data.
$AIC = 328.44$

Variable	$\hat{\beta}$	p-value	Rate ratio	95% confidence interval
(Intercept)	-2.25	< 0.0001	-	-
Slope	0.21	< 0.0001	1.23	1.14, 1.39
log(AADT HGV)	0.87	< 0.0001	2.38	1.98, 2.85

Table 24: Results from regression model of non-subsea tunnels.
Number of observations: 454, offset: Number of years with data and Length.
$AIC = 326.58$

A.3 Tunnels longer than 4 km

Variable	$\hat{\beta}$	p-value	Rate ratio	95% confidence interval
(Intercept)	-1.33	0.0885	-	-
log(Length)	0.99	< 0.0001	2.69	1.33, 5.45
log(AADT HGV)	1.27	< 0.0001	3.55	2.63, 4.78
Subsea	1.68	< 0.0001	5.37	3.01, 9.59

Table 25: Results from regression model of tunnels longer than 4 km.
Number of observations: 51, offset: Number of years with data.
$AIC = 100.14$

Variable	$\hat{\beta}$	p-value	Rate ratio	95% confidence interval
(Intercept)	-1.35	< 0.0001	-	-
log(AADT HGV)	1.27	< 0.0001	3.55	2.64, 4.78
Subsea	1.68	< 0.0001	5.39	3.11, 9.39

Table 26: Results from regression model of tunnels longer than 4 km.
Number of observations: 51, offset: Number of years with data and Length.
$AIC = 98.14$

A.4 Tunnels shorter than 4 km

Variable	$\hat{\beta}$	p-value	Rate ratio	95% confidence interval
(Intercept)	-2.03	< 0.0001	-	-
Slope	0.14	0.0011	1.15	1.06, 1.25
log(Length)	1.01	< 0.0001	2.75	1.80, 4.20
log(AADT HGV)	0.78	< 0.0001	2.18	1.79, 2.67

Table 27: Results from regression model of tunnels shorter than 4 km.
Number of observations: 434, offset: Number of years with data.
$AIC = 311.81$

Variable	$\hat{\beta}$	p-value	Rate ratio	95% confidence interval
(Intercept)	-2.03	< 0.0001	-	-
Slope	0.14	0.001	1.15	1.06, 1.25
log(AADT HGV)	0.78	< 0.0001	2.18	1.79, 2.66

Table 28: Results from regression model of tunnels shorter than 4 km.
Number of observations: 434, offset: Number of years with data and Length.
$AIC = 309.81$

References

2004/54/EC, D. (2004). Directive 2004/54/ec of the European Parliament and the Council of 29 april 2004 on minimum safety requirement for tunnel in the Trans-European Road Network.

AIBN (2013). RAPPORT OM BRANN I VOGNTOG PÅ RV23, OSLOFJORDTUNNELEN 23. JUNI 2011.

AIBN (2015). REPORT ON FIRE IN HEAVY GOODS VEHICLE IN THE GUDVANGA TUNNEL ON THE E16 ROAD IN AURLAND ON 5 AUGUST 2013.

AIBN (2016a). REPORT ON COACH FIRE IN THE GUDVANGA TUNNEL ON THE E16 ROAD IN AURLAND ON 11 AUGUST 2015.

AIBN (2016b). REPORT ON FIRE IN TANK TRAILER IN THE SKATESTRAUM TUNNEL IN SOGN OG FJORDANE ON 15 JULY 2015.

AIBN (2017). RAPPORT OM BRANN I VOGNTOG PÅ RV7 I MÅBØTUNNELEN 19. MAI 2016.

AIBN (2018). REPORT ON FIRE IN HEAVY GOODS VEHICLE IN THE OSLOFJORD TUNNEL ON NATIONAL ROAD 23 ON 5 MAY 2017.

Bjelland, H. and Njå, O. (2012). Interpretation of safety margin in aset/rset assessments in the norwegian building industry. In Proceedings to PSAM11 and ESREL 2012.

Carvel, R. and Beard, A. (2005). *The Handbook of tunnel fire safety*, Thomas Telford Ltd.

Cengel, Y. A., Cimbala, J. M. and Turner, R. H. (2012). *Fundamentals of Thermal-Fluid Sciences*, The McGraw-Hill Companies, Inc.

Dahle, G. H. (2005). *Tunnelbrann, dokumentasjon og korrupsjon [Tunnel fire, documentation and corruption]*, G. H Dahle.

Dobson, A. J. and Barnett, A. G. (2008). *An Introduction to Generalized Linear Models, 3rd ed.*, Chapman and Hall/CRC.

Drysdale, D. (1999). *An Introduction to Fire Dynamics*, John Wiley and Sons Ltd.

Elvik, R. and Mysen, A. (1999). Incomplete Accidents Repporting: Meta-Analysis of Studies Made in 13 Countries, pp. 133–140. Transportation Research Record(1665).

Eric W. Weisstein (2019). Lambert W-Function, `http://mathworld.wolfram.com/LambertW-Function.html`. Accessed: 02.05.2019.

FIVE (2019). `https://firesinvehicles.com/history/`. Accessed: 02.06.2019.

Hurley, M. (2016). *SFPE handbook of fire protection engineering*, Springer Publishing.

Høye, A., Nævestad, T.-O. and Ævarsson, G. (2019). Vegtunneler – branner, ulykker og havarier, TØI-rapport (in press).

Ingason, H., Li, Y. and Lönnemark, A. (2014). *Tunnel Fire Dynamics*, Springer Publishing.

Jackson, N., Pilley, A. and Owen, N. (1990). Instantaneous Heat Transfer in a Highly Rated DI Truck Engine.

Kleppe, T. S. (2015). Additional lecture notes for STA600, Lecture notes.

KS2 (2011). Rv. 13 Ryfast, E39 Eiganestunnelen og forlengelse av Nord-Jæren pakken.

Langeland, T. . (2009). Language and change: an inter-organisational study of the zero vision in the road safety campaign. (PhD). No. 72.

Lönnermark, A. (2007). Goods on HGVs during Fires in Tunnels.

Mikkelsen, R. (2018). Kkvm. Power Point presentations.

Minitab support team (2019). Residual plots for fit poisson model, `https://support.minitab.com/en-us/minitab/18/help-and-how-to/modeling-statistics/regression/how-to/fit-poisson-model/interpret-the-results/all-statistics-and-graphs/residual-plots/`. Accessed: 14.02.2019.

Njå, O. (2017). Hvordan tilnæme seg sannsynlighetsangivelse for branner i tunge kjøretøy i vegtunneler? Arbiedsnotat.

Njå, O., Jakobsen, E. and Nesvåg, S. (2008). *Høyrisikogrupper i vegtrafikken. Identifisering av undergrupper.*

Njå, O. and Kuran, C. (2015). *Erfaringer fra redningsarbeidet og selvredningen ved brannen i Oslofjordtunnelen 23. juni 2011 [Experiences from the resuce work and the self rescue in the Oslofjord tunnel fire 23 June 2011]*, International Research Institute of Stavanger.

Njå, O. and Svela, M. (2018). A review of the competencies in tunnel fire response seen from the first responders' perspective. Fire Safety Journal, 97.

Nævestad, T.-O. and Meyer, S. (2013). A survey of vehicle fires in Norwegian road tunnels 2008-2011.

R-Forge (2019). Residuals in glm, `https://r-forge.r-project.org/scm/viewvc.php/*checkout*/pkg/BinomTools/inst/ResidualsGLM.pdf?revision=6&root=binomtools&pathrev=6`. Accessed: 18.03.2019.

Statens vegvesen (2019). Statens vegvesen vegkart, `https://www.vegvesen.no/vegkart/vegkart/#kartlag:geodata/@600000,7225000,3`. Accessed: 12.03.2019.

Stec, A. and Hull, R. (2010). *Fire Toxicity*, Oxford: CRC Press.

SVV (2006). *Håndbok 021, Vegtunneler [Handbook 021 Road Tunnels]*, Statens vegvesen.

SVV (2016). *Håndbok N500 Vegtunneler [Handbook N500 Road Tunnels]*, Statens vegvesen.